Super-resolution microscopies, technological breakthrough to decipher mitochondrial structure and dynamic.

Pauline Teixeira, Rémi Galland, Arnaud Chevrollier

Seminars in Cell and Developmental Biology 159–160 (2024) 38–51

Contents lists available at ScienceDirect

Seminars in Cell and Developmental Biology

journal homepage: www.elsevier.com/locate/semcdb

Review

Super-resolution microscopies, technological breakthrough to decipher mitochondrial structure and dynamic.

Pauline Teixeira [a], Rémi Galland [b], Arnaud Chevrollier [a,*]

[a] Univ. Angers, INSERM, CNRS, MITOVASC, Equipe MITOLAB, SFR ICAT, F-49000 Angers, France
[b] Univ. Bordeaux, CNRS, Interdisciplinary Institute for Neuroscience, IINS, UMR 5297, F-33000 Bordeaux, France

ARTICLE INFO

Keywords:
Mitochondria
Nucleoids
Microscopy
Super-resolution
MICOS

ABSTRACT

Mitochondria are complex organelles with an outer membrane enveloping a second inner membrane that creates a vast matrix space partitioned by pockets or cristae that join the peripheral inner membrane with several thin junctions. Several micrometres long, mitochondria are generally close to 300 nm in diameter, with membrane layers separated by a few tens of nanometres. Ultrastructural data from electron microscopy revealed the structure of these mitochondria, while conventional optical microscopy revealed their extraordinary dynamics through fusion, fission, and migration processes but its limited resolution power restricted the possibility to go further. By overcoming the limits of light diffraction, Super-Resolution Microscopy (SRM) now offers the potential to establish the links between the ultrastructure and remodelling of mitochondrial membranes, leading to major advances in our understanding of mitochondria's structure-function. Here we review the contributions of SRM imaging to our understanding of the relationship between mitochondrial structure and function. What are the hopes for these new imaging approaches which are particularly important for mitochondrial pathologies?

1. Introduction

Mitochondria are multifunctional organelles involved in the control of a broad number of cellular functions, including energy production, metabolism, and different cellular responses. Recent findings show that mitochondria play an important role in many diseases such as neurodegenerative and metabolic disorders. Nowadays, the molecular mechanisms linking mitochondrial structure and dynamics to their physiological roles are progressively being revealed allowing us to envision a better understanding and possibly the development of new treatments.

The structural study of mitochondria by transmission electron microscopy (EM) in the 1950s has revealed the ultrastructural organisation of mitochondria with an outer membrane that covers an inner membrane forming invaginations called cristae. This inner membrane carries the oxidative phosphorylation complexes (OXPHOS) responsible for mitochondrial ATP production. OXPHOS activity is based on an assembly of many subunits that form four complexes, of which three are involved in proton (H^+) transfer (I, III, and IV). The F1F0-ATP synthase, using the H^+ gradient to produced ATP, can be considered as complex V. More recently, it has been shown that these complexes contribute to membrane folding leading to the specific shape of the cristae [1,2] such as the dimerisation of F1F0-ATP synthase which induces membrane curvature at the cristae tips [3–5]. Transmembrane electrostatic proton localisation model also showed that by increasing the membrane surface area, the formation of cristae would be energetically favourable to increase the energy storage [6], linking the mitochondria ultrastructure to one of its major functions.

Abbreviations: CSM, Confocal Scanning Microscopy; DNA-PAINT, DNA-based Point Accumulation for Imaging in Nanoscale Topography; DRP1, dynamin-related protein 1; EM, electron microscopy; ER, endoplasmic reticulum; MAM, mitochondria-associated membrane; MFN1/MFN2, mitofusin 1/mitofusin 2; MICOS, mitochondrial contact site and cristae organising system; MINFLUX, MINimal photon FLUXes; MOMP, mitochondrial outer membrane permeabilization; mtDNA, mitochondrial DNA; Myo19, myosin 19; ΔΨm, mitochondrial membrane potential; NL-SIM, non-linear illumination patterns; OPA1, optic atrophy 1; OXPHOS, oxidative phosphorylation; PA-FP, photo-activable fluorescent protein; PALM, PhotoActivation Localisation Microscopy; RESOLFT, REversible Saturable OpticaL Fluorescence Transition; ROS, Reactive Oxygen Species; SIM, Structured Illumination Microscopy; SMLM, Single Molecule Localisation Microscopy; SPT, Single particle tracking; STED, STimulated Emission Depletion; dSTORM, (direct) Stochastic Optical Reconstruction Microscopy; TIRF, Total Internal Reflection Fluorescence.

* Corresponding author.
E-mail address: arnaud.chevrollier@univ-angers.fr (A. Chevrollier).

https://doi.org/10.1016/j.semcdb.2024.01.006
Received 11 October 2023; Received in revised form 8 January 2024; Accepted 25 January 2024
Available online 3 February 2024

Mitochondria are ubiquitous organelles in eukaryotic cells. Their endosymbiotic origin from an alphaproteobacterium partly explains their current structural and genetic specificities (reviewed in [7]). Notably, mitochondria have kept the particularity to possess their own circular genome, called the mitochondrial DNA (mtDNA). Human mtDNA is 16,569 base pairs long and is organised in nucleoprotein complexes called nucleoids, present in hundreds per cell, and distributed throughout the mitochondrial network. The mtDNA codes for 13 proteins which are all needed for the OXPHOS complex. Therefore, it is not surprising that the first descriptions of cristae structure came from a cell type that was depleted of mtDNA (ρ0 cells) [8]. However, additional factors are essential for mitochondrial structuring. The bending of the inner membrane was also shown to depend on phospholipid composition in particular cardiolipin, phosphatidylethanolamine and phosphatidylcholine [9]. High resolutive electron tomography and focused ion beam-scanning electron microscopy (FIB-SEM) have made it possible to obtain ultrastructural representation of mitochondrial sheets and cristae in 3D. Indeed, behind the classic image of the mitochondrion in the shape of a bean with its parallel cristae filling the matrix, EM revealed a wide diversity of mitochondria shapes depending on the tissue [10–12], and damage linked to the structure and/or the OXPHOS genes [13]. Nevertheless, due to EM restricted image areas, representativeness at intracellular and inter-cellular levels has remained limited.

The development of optical microscopy, and in particular the advent of genetically encoded fluorescent proteins (e.g. GFP) [14] has made it possible to show the incredibly dynamic behaviour of mitochondria inside cells [15]. Mitochondria can move within the cell via the cytoskeleton [16], but also fuse with each other or split apart [17], resulting in the formation of either long or more fragmented networks depending on the cellular functions [18]. Fusion is mainly orchestrated by optic atrophy 1 (OPA1) for the inner membrane and mitofusin 1 and 2 (MFN1 and MFN2) for the outer membrane [19], while fission is regulated by dynamin-related protein 1 (DRP1) [20]. Mitochondria are also closely linked to or physically connected to other organelles of the cell, in particular with the endoplasmic reticulum (ER), which participates in the constriction of mitochondria and thus in the control of mitochondrial fission [21].

In most of the cells, mitochondria are between 200 and 500 nm in diameter, close to or below the resolution limit that can be achieved by conventional fluorescent microscopy, which is ≈ 300 nm in the radial (XY) direction and ≈ 700 nm in the axial (Z) direction. Therefore, for several decades, the nanoscopic study of mitochondrial ultrastructure was thus only possible by EM, which offer excellent resolution but suffers from technical bias. To encompass these, cryo-fixation, by means of high-pressure freezing, has recently improved the high-fidelity ultrastructural imaging [22]. Nevertheless, most of the published data still comes from chemical fixatives that damage or modify the cristae. Additionally, the volumes that can be probed by EM are restricted to micrometre scales down to a few hundreds of nanometres axially, limiting the overall field of view achievable. Moreover, EM usually lacks the specificity that can be achieved in fluorescence microscopy and its capacity to strictly label only one or several biomolecules of interest. Lastly, despite its high magnification, EM only allows static observation on fixed tissues.

The development of Super-Resolution fluorescent Microscopy (SRM) techniques, allowing to go beyond the light diffraction barrier, has enabled crucial advances in different fields of research in biology [23]. It enabled to reveal the organisational level and structure of many

Table 1
Super-resolution microscopy (SRM) techniques.

Techniques		Radial (d_{xy}) and axial (d_z) spatial resolution (nm)	Temporal resolution (Hz)	Advantages	Limitations	Refs
SIM	SIM	$d_{xy} \approx 120, d_z \approx 350$	1 – 250	- Common fluorophore - High sensitivity - Live imaging compatible - High temporal resolution	- Limited resolution gain - Reconstruction artefact	[36]
	NL-SIM	$d_{xy} \approx 60, d_z \approx 200$	n.a.	- Improved resolution gain	- High Power laser - Reconstruction artefact	[36]
	ISM	$d_{xy} \approx 120, d_z \approx 350$	1 – 30	- Common fluorophore - High sensitivity - Live imaging compatible - 3D optical sectioning - High temporal resolution	- Limited resolution gain	[43]
STED	STED	$d_{xy} \approx 50, d_z \approx 80$	0.1 – 10*	- High spatial resolution - Allows 3D imaging	- High power laser - Limited field of view - Photostable fluorophores - Limited temporal resolution - Potentially Complex implementation	[182]
	WF-RESOLFT MoNaLISA	$d_{xy} \approx 70, d_z \approx 100$	1	- High spatial resolution - Allow 3D imaging - Live imaging compatible	- Photo-switchable fluorophores - Complex implementation	[47]
SMLM	PALM	$d_{xy} \approx 30, d_z \approx 80$	0.01 - 1	- High spatial resolution - Live imaging compatible - Protein's quantification	- Photo-switchable fluorophores - Limited temporal resolution	[50]
	dSTORM	$d_{xy} \approx 10, d_z \approx 50$	n.a.	- Very high spatial resolution - Multi-colour capabilities	- Specific fluorophore - Live incompatible	
	DNA-PAINT	$d_{xy} \approx 10, d_z \approx 50$	n.a.	- Very high spatial resolution - Protein's quantification - Multi-colours capabilities		
	sptPALM	$d_{xy} \approx 30, d_z \approx 80$	50**	- High spatial resolution - Live imaging compatible - High statistics	- Photo-switchable fluorophores	
MINFLUX		$d_{xy} \approx 1, d_z \approx 2$	1000**	- Extremely high spatial and temporal resolution - Live imaging compatible	- Limited field of view - Lack of availability up to now	[39]

Review Super-resolution microscopies, technological breakthrough to decipher mitochondrial structure and dynamic.
* Depend on the field of view size;
** Record single molecule dynamics

complexes such as the nuclear pores [24], the cytoskeleton [25,26] or the chromatin compaction within the nucleus [27]. With a spatial resolution down to a few nanometres (Table 1) and the specificity of fluorescence-based microscopy, these techniques pave the way towards a better comprehension between the (ultra-)structures and the functions of proteins complexes and/or organelles. In mitochondrial research, SRM and the use of fluorophores specifically targeting mitochondrial compartments now make it possible to study the nanoscale organisation and dynamics of outer membranes, inner membranes and even matrix components such as the nucleoid. Furthermore, SRM allows to observe interactions of mitochondria with other components of the cell such as the ER, lysosomes [28] and cytoskeleton [29]. In addition, the compatibility of SRM with live observation creates the opportunity to study the highly dynamic nature of these organelles at the nanoscale.

The increasing availability and simplification of these systems makes now possible to obtain new images and insights about the behaviour of mitochondria in all areas of interest. These new technologies represent a real breakthrough in research into multiple pathologies linked to mitochondria, such as neurodegenerative diseases, cardiovascular diseases, and cancer. Indeed, mitochondrial dysfunction is one of the hallmarks of cancer, along with escape from apoptosis and bioenergetic deregulation [30], emphasising the need to better understand the mechanisms of structural organisation of mitochondrial networks, inner membrane remodelling and mitochondrial shape plasticity [31]. In a pathological context, the fate of damaged mitochondria or mitochondrial residues is currently the subject of considerable attention due to the importance of these elements as secondary messengers able to activate stress pathways. It is therefore essential to be able to observe with greater resolution the events that lead to mitochondrial damage [32] such as mitochondria-derived vesicles (MDV) that bud off and then transit to lysosomes or nanotube-mediated transfer of mitochondria from immune cells to cancer cells in order to improve future treatments (review to evaluate mitochondria in cancer [33]).

2. Super-resolution microscopy (SRM) techniques

Fluorescent microscopy is a very active multidisciplinary field combining optics, chemistry, physics, and biology. New techniques and staining strategies are emerging all the time [14], especially driven by several commercial partners facing strong pressure to bring out the best tools capable of surpassing previous limits and making them accessible to different research areas. However, fluorescence microscopy spatial resolution is intrinsically limited by the light diffraction phenomenon, through which a single emitter appears as a diffraction pattern, called Point Spread Function (PSF), onto the camera with a diameter of $\approx \lambda/2NA$, where λ is the wavelength and NA the numerical aperture of the objective [34]. Consequently, any object smaller than this distance, around 200 - 300 nm radially and 500 - 700 nm axially, cannot be resolved, thus preventing the precise observation of fine structures, such as mitochondria, and its ultrastructure inside cells (Fig. 1A).

SRM defines microscopy techniques that overcome this limit imposed by the diffraction of the light and enable to achieve spatial resolution down to a few nanometres radially and axially. Awarded in 2014 by the Nobel Prize in Chemistry, it encompasses four main families of techniques: Structured Illumination Microscopy (SIM) [35,36], STimulated Emission Depletion (STED) [37,38], Single Molecule Localisation Microscopy (SMLM), and MINimal photon FLUXes (MINFLUX) [39]. Each family of techniques is based on a different approach to overcome the diffraction limit and thus separate points closer than $\approx$ 200 nm [40] (Table 1 and Fig. 1). Nevertheless, they all mainly rely on an accurate control of the emission properties of the fluorophores to extract additional information from their emission pattern.

2.1. SIM

In SIM imaging, the excitation light is spatially structured to make normally inaccessible high spatial frequency information contained in the sample, accessible in the form of a Moiré pattern. Those high spatial frequencies correspond to the fine details of an image, but are usually blurred by the microscope PSF, leading to the resolution limit of optical microscopes. When illuminating the sample with a structured illumination (usually sinusoidal), the sample's spatial frequencies are convolved with the ones of the illumination pattern creating a so-called Moiré pattern. This Moiré pattern contains information about the very fine details (or high spatial frequencies) of the samples, that a regular microscope cannot detect under regular illumination. The principle of SIM is then to extract those high spatial frequencies from the detected Moiré patterns by image processing, in order to reconstruct an image with an improved spatial resolution [35,41] either in 2D, or in 3D when a 3D grid-like illumination pattern is used [42] (Fig. 1B). This reconstruction requires the acquisition of at least 9 images in 2D with different positions and orientations of the illumination pattern. While for 3D SIM, a minimum of 15 images needs to be acquired. It commonly leads to a spatial resolution improvement of $\approx$ 2, namely $\approx$ 120 nm radially and $\approx$ 350 nm axially. It can be further improved using non-linear illumination patterns (NL-SIM) containing higher spatial frequencies but at the expense of much higher illumination doses potentially harmful to the samples [36].

SIM imaging has the advantage of being compatible with all existing fluorophores and labelling techniques. Furthermore, it has a high sensitivity and enables to remove the out-of-focus light improving the overall image contrast, while requiring a minimal excitation light's dose. It thus makes this technique ideal for live sample imaging with imaging rate up to $\approx$ 250 Hz [29] (see Section 10). However, SIM imaging can easily be prone to image reconstruction artefacts, since the final reconstructed image quality depends on the capacity to extract the high spatial frequencies from the potentially complex and noisy Moiré patterns created. Finally, other illumination patterns, such as point illumination used in Confocal Scanning Microscopy (CSM) or speckle patterns, can also be used for SIM imaging. In the case of point illumination, a 2D array detector is used to collect the signal instead of a single pinhole as in CSM. It gives the possibility to re-assign the photons collected on each pixel to their effective emission position leading to a spatial resolution improvement [43] similar to standard SIM. Those methods (ISM, RCM, AiryScan) (Table 1), and their alternative that parallelise the excitation spots (MSIM, ISIM), enable to conserve the optical-sectioning ability of CSM while improving the final spatial resolution by $\approx$ 2.

2.2. STED

STED microscopy is a point-based scanning technique where an excitation spot is scanned throughout the sample to create a 2D image similarly to CSM. In CSM, the excitation spot is subjected to the light diffraction leading to a minimum excitation area of $\approx$ 200 - 300 nm limiting the final spatial resolution. Whereas in STED microscopy, this emission area is narrowed thanks to an additional "doughnut"-shaped laser beam superposed to the excitation beam, which depletes, or de-excites, the fluorescence emission outside from its centre. Consequently, this limits the effective fluorescence emission area and increases the achievable spatial resolution (Fig. 1C). The laser intensity of the "doughnut"-shaped laser beam determines the size of its hole at the centre and thus the emission area. However, in practice, too high laser intensity leads to increased photobleaching and phototoxicity which limits the application of STED microscopy to live sample and the achievable spatial resolution to $\approx$ 50 nm [44]. In addition, as with all point scanning techniques, the temporal resolution of STED microscopy is relatively slow, and trade-offs must be made between the field of view size and acquisition time. To overcome these limitations, it has been proposed to use reversible photo-switchable fluorescent proteins to reduce by several order of magnitude the light dose required to control the *On/Off* emission states of the fluorophores. It allows to achieve sub

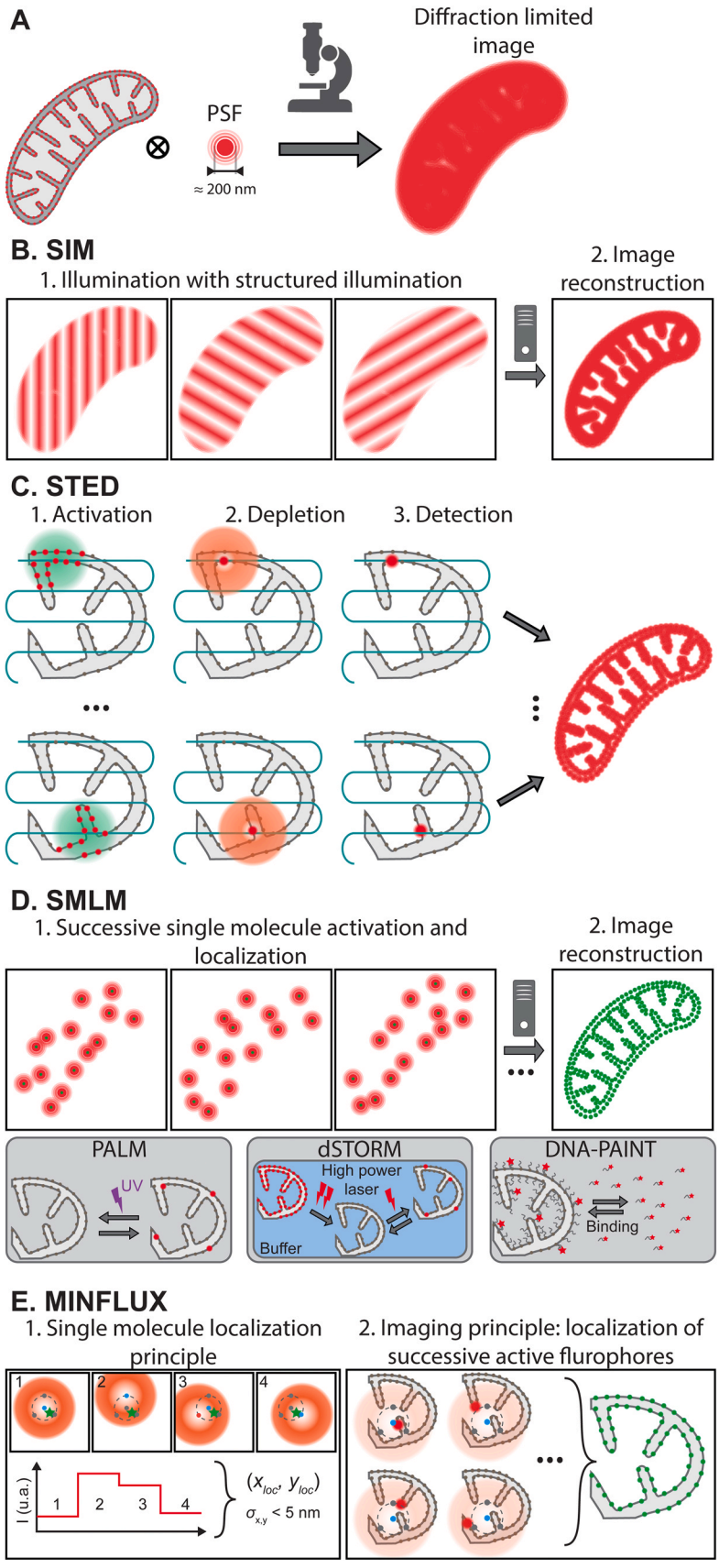

(caption on next page)

Fig. 1. Principle of main super-resolution microscopy (SRM) techniques. (A) Principle of image formation through an optical microscope. When a single emitter (fluorophore) is imaged through a microscope, it creates a diffraction pattern, called the microscope's Point Spread Function (PSF), having a size of ≈ 200 nm. The image of a distribution of fluorophores through a microscope is therefore the convolution of this distribution with the microscope's PSF blurring the actual emitter's distribution and thus limiting the achievable spatial resolution. (**B**) Structured Illumination Microscopy (SIM) principle. The sample is illuminated with a structured illumination having high spatial frequencies. This shifts the spatial frequencies of the fluorophores spatial distribution making accessible some previously inaccessible frequencies through the objective. Combining several orientations and positions of the excitation pattern, it enables to reconstruct a super-resolved image. Spatial resolution: ≈ 120 nm radially and ≈ 350 nm axially. (**C**) STimulated Emission Depletion (STED) microscopy principle. A diffraction limited excitation spot is used to excite a ≈ 200 nm area in a sample. A doughnut-shaped laser beam is then superposed to deplete the fluorescence emission outside of its centre, narrowing the fluorescence emission area. This process is repeated throughout the entire sample to produce a super-resolved image. Spatial resolution: ≈ 50 nm radially and ≈ 80 nm axially. (**D**) Single Molecule Localisation Microscopy (SMLM) principle. Only a sparse subset of the fluorophore is activated at each frame so that their PSF are spatially isolated and can be precisely localised (green dots). Repeating this process thousands of times, and pooling all the single molecule localisation all together, it allows to reconstruct a super-resolved image. Spatial resolution: ≈ 20 nm radially and ≈ 50 nm axially. This sparse activation can be done either optically using UV light (PALM), by controlling the photophysics of fluorophores through a high-power laser and a specific buffer (dSTORM) or relying on the transient binding of complementary DNA strands (DNA-PAINT). (E) MINimal photon Fluxes (MINFLUX) microscopy principle. A doughnut-shaped laser beam is used to achieved a near molecular localisation of isolated fluorophores thanks to a triangulation-like techniques based on the fluorophore emission according to 4 successive laser spot positions. To form a super-resolved image, this process combined the sparse activation of the fluorophore from SMLM and the doughnut-shaped laser beam localisation method. Spatial resolution: ≈ 2 nm radially and axially.

100 nm spatial resolution within living samples in a technique called REversible Saturable OpticaL Fluorescence Transition (RESOLFT) [45]. Widefield alternative to STED microscopy, such as WF-RESOLFT [46] and MoNaLISA [47] have also been proposed to increase the achievable temporal resolution down to ≈ 1 Hz by creating many parallel excitation and depletions spots. It has to be noted that all those techniques have been extended in 3D thanks to the patterning of the depletion beam in 3D, leading to axial resolution down to ≈ 80 nm [38,48]. Finally, deep learning method based on image restoration approaches has recently been proposed to further reduce the light dose of STED like microscopies and increase the achievable temporal resolution [49].

2.3. SMLM

SMLM techniques rely on the capacity to localise the position of a single emitter with a much greater accuracy than the light diffraction, assuming its PSF is spatially isolated onto the detector. In SMLM imaging, the fluorophore emissions are separated in time through their sequential activation between a dark (or *Off*) and a bright (or *On*) state. This creates a blinking effect so that each fluorophore's PSF can be spatially isolated at any given time. The centre of each PSF is then computationally localised with a precision of a few nanometres. This operation is repeated for thousands of frames, until, ideally, that all the fluorophores have been detected and localised. A super-resolved image is finally reconstructed by pooling all the localisations computed on each frame [50] (Fig. 1D). Typical resolution achieved in SMLM is ≈ 20 nm radially and ≈ 50 nm axially when 3D localisation methods are used. Nevertheless, this resolution depends on the precision at which the fluorophores are localised and the total number of localisation [51]. SMLM includes several techniques depending on the strategies developed to allow the switching *On/Off* of the fluorophores. PhotoActivation Localisation Microscopy (PALM) [52,53] uses UV light to activate the fluorophore emission. Stochastic Optical Reconstruction Microscopy (STORM) [54] and direct STORM (dSTORM) [55] rely on the control of the photophysical properties of the fluorophore. And Point Accumulation for Imaging in Nanoscale Topography (PAINT) [56–58] and its variant DNA-PAINT [57] uses the transient (or not) binding of fluorophores diffusing in the media to the proteins of interest.

By using genetically encoded photo-activable fluorescent proteins (PA-FPs), PALM related techniques offer the advantages of being compatible with living samples and stoichiometry studies, but at the expense of slightly lower spatial resolution due to the use of dimmer dyes. By using bright organic fluorophores, dSTORM techniques enable more accurate localisation and therefore spatial resolution. However, the need to introduce those dyes into cells and the control of their photophysical properties (high-power laser and chemical buffer) generally restricts their use to fixed samples. Finally, PAINT techniques, and especially DNA-PAINT approaches, combine the advantages of using bright organic fluorophores for improved spatial resolution and of being insensitive to their irreversible photo-bleaching as the medium acts as an infinite reservoir of imagers. However, DNA-PAINT imaging is mostly restricted to fixed samples and requires higher acquisition time due to the relatively slow binding-unbinding kinetics of DNA complementary strands.

Last but not least, SMLM super-resolution methods encompass also Single Particle Tracking methods (SPT) that allow to record the dynamics of single proteins. Indeed, if a single isolated fluorophore is detected over several consecutive frames, it becomes possible to link all its localisation to reconstruct its trajectory. Using PA-FPs, it becomes possible to detect the trajectory of many dyes leading to statistically relevant analysis of proteins dynamics in a technique called sptPALM [59], and consequently to reveal important insights in the dynamics of the proteins of interest [60].

2.4. MINFLUX

More recently, a fourth SRM family has been developed called MINFLUX which combines the stochastic emission of single isolated fluorophores of SMLM with their coordinate targeted localisation of STED microscopy using a "doughnut"-shaped laser beam [39]. When illuminating a single fluorophore with such a beam its very accurate localisation can be achieved through triangulation approach knowing very precisely the position of the beam (Fig. 1E). This method allows to localise single molecules with isotropic resolution down to a couple of nanometres [61] at a rate of few kHz and with minimal photon emission from the fluorophore. It leads to the possibility to record proteins distribution with true molecular resolution, tracking proteins over extended time windows and providing an impressive insight into their dynamics [62]. A major limitation of MINFLUX is however the restricted field of view of few micrometres that can be probed and its limited availability as for now.

2.5. SRM limitations and perspectives

Despite the many efforts in SRM field in the past two decades, several limitations remain. One limitation is their ability to perform precise stoichiometry studies of proteins of interest. STED and SIM approaches give insight in bulk information in which absolute proteins copy number cannot be extracted. SMLM approaches have theoretically this capacity, however complex fluorophores photo-physics (i.e. bleaching, blinking, …) as well as labelling stoichiometry makes this task particularly challenging. In addition, it also raises the important task of labelling the endogenous proteins while ensuring a minimal impact on the function of the proteins of interest.

A second limitation of SRM techniques are their acquisition time and potential photo-toxic effects that can impede the possibility to probe

dynamic events of structures such as mitochondria within living samples. Indeed, as in any microscopy modalities, trade-offs must be made in between the achievable (i) spatial resolution, (ii) temporal resolution and (iii) the required illumination dose. The capacity of SRM to break the diffraction barrier has therefore been possible but only at the expense of the two other capacities. Nevertheless, amongst SRM techniques, SIM-based approaches are surely the best suited to observe ultrastructure remodelling events thanks to their widefield acquisition schemes and their rapid acquisition modalities requiring lower doses of light but at the expense of a limited spatial resolution gain. On the other hand, sptPALM, and more recently MINFLUX, offer the capacity to probe single proteins dynamics up to 0.01 – 0.1 $\mu m.s^{-1}$ [63] at higher resolution but failed to report bulk information and over usually lower field of views.

Finally, a last SRM limitation is the capacity to image in depth within 3D samples such as 3D cell cultures or tissues. Indeed, the illumination structuration of SIM, STED and MINFLUX techniques tends to get blurred with depth due to sample-induced absorption, scattering and optical aberrations. Specific applications such as ISM-like approaches, two-photons based STED, or adaptive optics-based correction may be used to increase the penetration depth, but at the expense of more complex implementation. In SMLM, efficient light collection through high Numerical Aperture (NA) objectives and optical sectioning approaches that confine the excitation light to the imaged plane are required to allow the accurate detection and localisation of single molecule. It therefore mostly limits the imaging capacity to the first microns above the coverslips using Total Internal Reflection Fluorescence (TIRF) or Highly Inclined Illumination (HILO) excitation schemes [64]. In the last decades, several attempts were made to increase the penetration depth of SMLM approaches, mostly using dedicated Light-Sheet (LS) excitation architectures compatible with the use of high NA objectives such as Lattice Light Sheet microscopy [65], single-objective based architectures [66], or tilted light-sheet geometries [67]. This capacity to probe the nanoscale organisation of proteins in depth within 3D cell cultures or tissues might bring unprecedent insights of mitochondrial functions in more physiological conditions.

2.6. *The difficult task to choose the appropriate SRM technique*

The diversity of SRM techniques offers many possibilities for observing the ultrastructure of organelle, such as mitochondria, and proteins distribution with resolution down to a few tens of nanometres. It also allows to probe the dynamics of either protein structures (SIM, STED) or individual proteins (SMLM, MINFLUX) providing unprecedent insights in the structure-function relationship of biological complexes and/or organelles. STED and SIM imaging are typically used to observe the inner structures of mitochondria as well as their remodelling dynamics (fission and fusion events, cristae remodelling processes,…) [68,69], whereas SMLM and MINFLUX can be used to decipher the nanoscale organisation of proteins and biomolecules within mitochondria and their individual dynamic behaviours. The aim of the technical description in this section was (i) to provide the basic principle of the different SRM modalities, and (ii) to propose some rough comparison elements, summarised in Table 1, to help users to choose the appropriate SRM techniques that would fulfil their needs according to their biological questions and therefore the spatial and temporal resolution they need. It is interesting to note that the study of mitochondria was one of the first biological targets for the development of SRM techniques, whether it was for bulk imaging approaches (SIM and STED) [70], or for single molecule targeted ones (SMLM and MINFLUX) [52]. It exemplifies the importance of going beyond the resolution limit to study mitochondria, their ultrastructure, composition and remodelling pathways. With these new techniques, SRM has and will continue to provide major contributions to the mitochondrial field.

3. SRM specified the number of mtDNA per nucleoid and their distribution within the mitochondria

MtDNA and its maintenance by factors that make up the nucleoid, such as twinkle or TFAM are essential for the structural and functional integrity of mitochondria and thus for cellular homeostasis (Fig. 2). Numerous pathologies linked to defects in mtDNA maintenance have been demonstrated, such as mtDNA depletion syndromes (for review [71]), neurodegenerative diseases (for review [72]) or myopathies (for review [73]). Exploring the nucleoid in terms of its composition, structure and location seems essential for a better understanding of these pathologies.

MtDNA content, assessed by molecular biology technologies such as quantitative PCR, revealed a wide range of copy between cells. By evaluating the mtDNA copy number by quantitative PCR in relation to the number of nucleoids seen by immunofluorescence, Legros *et al.* have first identified in primary and immortal human cell lines between 2 and 8 mtDNA molecules per nucleoid [74]. However, the different groups interested in nucleoids highlight a certain number of undetected nucleoids due to the limitations of the technique and in particular some targets that are too small to be observed by wide-field fluorescence and confocal microscopy [74,75]. Hence, it became apparent that neither the mtDNA copy number per nucleoid nor the nucleoid size could be accurately assessed by conventional light microscopy.

STED microscopy provided new images of nucleoids in fibroblasts, showing 1,800 nucleoids per cell for human fibroblasts and predicting an average of 1.4 mtDNA molecules per nucleoid [76,77] suggesting almost a single copy of mtDNA per nucleoid. This number is still debated, as recently using dSTORM microscopy Pavluch *et al.* would adjust this value to 2.07 mtDNA molecules per nucleoid [78]. This data would be an intermediate value if we take into account the data from Brown *et al.* with 3 mtDNA molecules per nucleoid with PALM (2D) and iPALM (3D) [60]. This diversity of mtDNA content could be associated with the diversity of nucleoid shapes and sizes. By STED, Kukat *et al.* showed an ellipsoidal structure of the nucleoid with a uniform size and on average a size of 100 nm diameter per nucleoid in seven different mammalian cell lines [76]. However, Brown *et al.* found a wide range of sizes between 31 and 318 nm per nucleoid using dSTORM and PALM imaging techniques [60]. The volume might reflect the compaction of mtDNA and therefore its accessibility for transcription factor. The nucleoid can be relatively big with a size reaching the diameter of the mitochondria. The high resolution of SRM and its capacity to target different object revealed that nucleoids are present in the void between cristae and can be in contact with them [79–81]. This close location could facilitate the insertion of respiratory chain protein by reducing the distance between the transcription site and where the proteins are needed. By the help of super resolution SIM, it has been recently shown that the major mtDNA-binding protein TFAM not only packages mtDNA within the nucleoid, but also drives mitochondrial nucleoid self-assembly in a phase separation model [82]. Phase separation of mitochondrial nucleoids recruits factors comprising the transcriptional initiation complex, elongation complex and termination factors in a co-phase separation manner [83]. This compartmentalisation concentrates the protein factors for more efficient transcription. Interestingly, while the nucleoid distribution was thought to be passive, it has been shown that mitochondrial-ER interaction is required for nucleoid distribution at the cell periphery with the implication of mitochondrial contact site and cristae organising system (MICOS) [84]. In addition, more recently, new data showed controlled expulsion of mtDNA under certain conditions of apoptosis or mitophagy, results that we will discuss later in the document (see Section 9). The difficulty of accurately quantifying the number of nucleoids per cell also lies in the complexity of identifying them within the 3D organisation of mitochondria in cells.

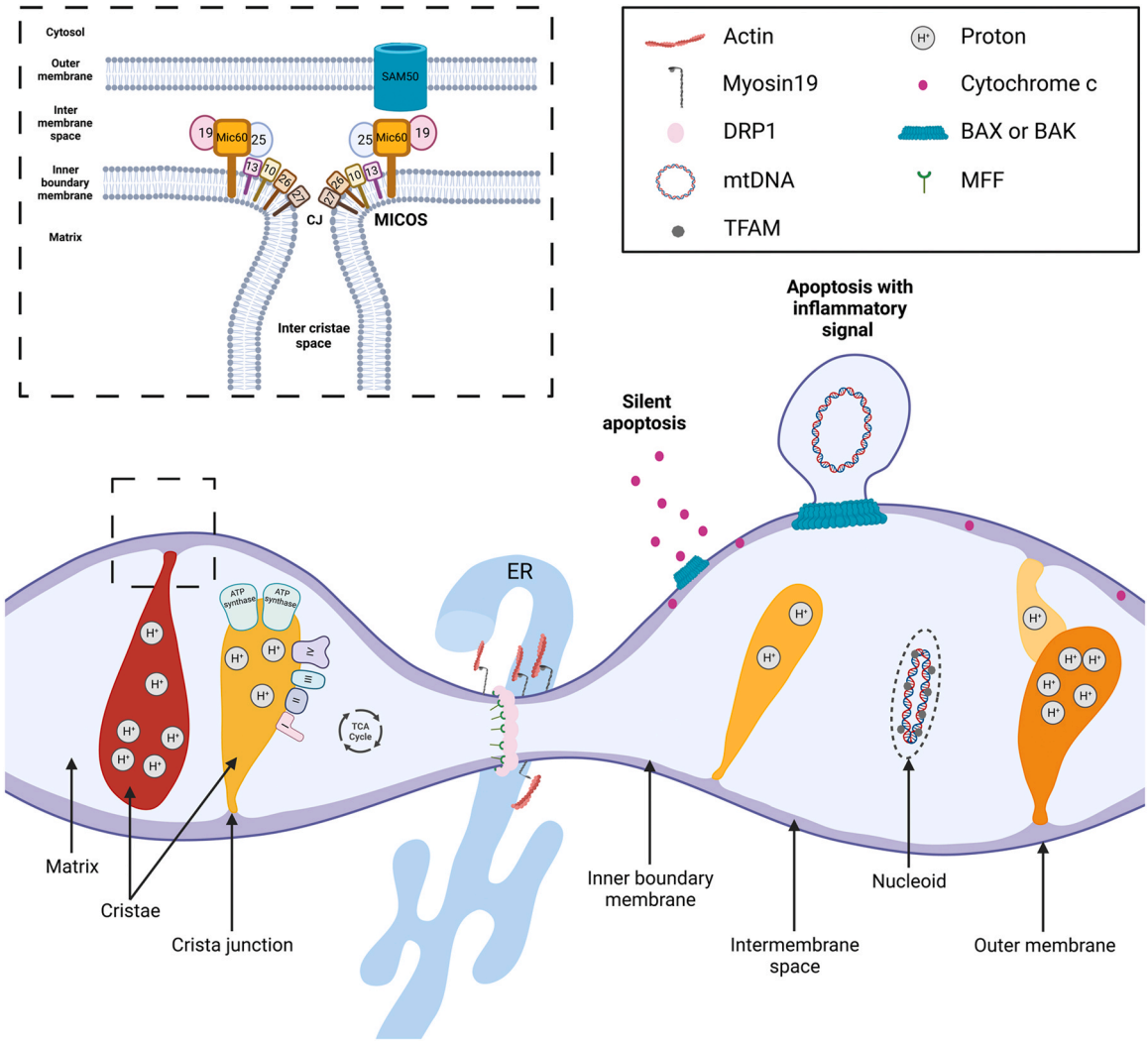

Fig. 2. Schematic illustration of mitochondrial structure and main mechanisms in mitochondrial dynamics studied and characterised in super-resolution microscopy. Mitochondrial fission through the ER-actin, Myo19 and DRP1 constriction, apoptosis signalling with BAX/BAK pores inducing the release of cytochrome c for the silent apoptosis or mitochondrial DNA for the apoptosis with inflammatory signal and mitochondrial membrane potential heterogeneity between cristae of one mitochondrion. The dot rectangle represents a zoom with the structural shaping of crista junction by the complex MICOS. CJ – crista junction; ER - endoplasmic reticulum; TCA cycle – tricarboxylic cycle; I-IV – OXPHOS complex I-IV.

4. SRM has improved the assessment of the mitochondrial network connectivity and mitochondrial fission sites

Mitochondrial dynamics is required for numerous mechanisms such as apoptosis, senescence, mitophagy, mitochondrial biogenesis and the metabolic status of cells (for review [85]). Their morphological changes are the result of continuous fusion and fission cycle that are extremely important for the maintenance of mitochondrial functions and cellular homeostasis. Mitochondrial dynamics are thought to be an essential process for the survival and regeneration of motor neurons after nerve damage, since disruption of these dynamics would lead to an acceleration of neurodegeneration [86]. Mutations in the main proteins in charge of the fusion and fission mechanism can result in neurodegenerative diseases [87] or severe antenatal encephalopathy, up to the point of lethality in children with DRP1 mutations [88] or MFN2 mutations [89]. In general, defects in mitochondrial dynamics are linked to multiple pathologies (review in [90]). The mitochondrial fission is a complex mechanism which requires several factors and interactions with at least the ER and actin filaments [91]. Mitochondrial fission factors (MFF) located on the mitochondrial outer membrane recruit the cytosolic factor DRP1 [92,93] which is considered as the main actor of the mitochondrial fission machinery (Fig. 2). DRP1 form a homomultimeric ring around the mitochondria and by its GTPase core can constrict and divide mitochondria [94]. SRM has enabled a better visualisation of the mitochondrial shape, size and diameter, as well as their inter-organelle interactions. While the fission site between mitochondria was thought to be random, with an unexplained difference between fission promoting mitophagy and fission promoting proliferation, the live SRM shed light on this mechanism. Indeed, with live-SIM it has been revealed that mitochondrial divisions occurring at the periphery, and resulting into small mitochondria, promote the mitophagy of damaged material and the shedding of nucleoid condensates induced by oxidative stress [95]. Whereas divisions in the middle of mitochondria drive their proliferation [96]. Both fission types would be mediated by DRP1 but only the fission leading to proliferation would require MFF and pre-constriction mediated by ER actin. As shown by STORM microscopy, other factors are involved in regulating fission, such as myosin 19 (Myo19), which is thought to act on mitochondria as a facilitator of actin binding, improving contacts between mitochondria and ER-associated actin prior to mitochondrial division [97]. Furthermore, through high spatial and temporal resolution N-SIM microscopy it has been shown in Hela cells that lysosomal contacts mark the sites of mitochondrial fission [98].

Lysosomes are recruited to the mitochondrial constriction site after the ER, and phosphatidylinositol-4-phosphate (PI(4)P) from lysosomes would be required for mitochondrial fission [99].

5. SRM has improved the evaluation of the contact points between the ER and mitochondria

Studying the relationship between the ER and mitochondria is tricky, given that both form complex, intertwined networks within cells. Through electron tomography ER and mitochondria have been shown to be separated from only 10 – 30 nm in various region, enough to consider these points as contact sites [100,101]. Contact sites ER-mitochondria, or mitochondria-associated membrane (MAM), are important to calcium homeostasis [21,102,103], phospholipid synthesis [104,105], insulin sensitivity and ROS homeostasis [106]. Disruption of these contact sites have been linked to several diseases such as amyotrophic lateral sclerosis (for review see [107]), aging (for review see [108]), diabetes or cancer (for review see [109]). The communication between ER and mitochondria received a great interest to identify biomarker and the development of targeted therapies [110]. Electron tomography and live imaging revealed that some ER tubules associate with mitochondrial constriction sites, followed by mitochondrial division, and this prior to the recruitment of DRP1 [101] (confirmed later by SRM [111]). Two hypothesis have been proposed: the first one is that ER tubules wrapping around mitochondria can constrict mitochondria exerting forces and help the division machinery to achieve the fission, the second one is that through its physical interaction the ER wrapping induces signalisation to the division machinery [101,111,112]. Live SRM with TIRF-SIM [29,113] and STED dual colour [114] have provided greater details than previously obtained by EM, by allowing to show the dynamic of ER wrapping around mitochondria but without being in capacity to validate any of these hypotheses. In another mechanism, in a context of ER stress, the MFN2 fusion protein was shown by SIM to increase the stability and lifetime of MAM. This increased MAM stability would promote the entry of Ca^{2+} into the matrix, increasing tricarboxylic acid (TCA) cycle activity and ATP production. Since the ER depends on a high amount of ATP to fulfil its functions, the rise of ATP supply to the ER may reduce its stress [115]. SRM imaging results are progressing with the development of suitable fluorescent probes showing the continuous progress and opening to new research on these interactions. Recently a novel ER marker called RR-mNeonGreen was demonstrated for SRM observation, compatible with live-cell and able to track the interaction between ER and mitochondria [116].

6. SRM has given new insight into the organisation of the cristae and the role of the subunits of the MICOS complex

The cristae are extensions of the inner membrane, forming folds to increase the membrane surface area available for positioning OXPHOS complexes. The identification of a protein complex called MICOS, which controls the anchoring of the cristae to the peripheral inner membrane, has reinforced the notion of structural and functional individualisation of the cristae (Fig. 2). MICOS [117] consists of at least 7 subunits in humans, Mic10 (MINOS1), Mic13 (QIL1), Mic19 (CHCHD3), Mic25 (CHCHD6), Mic26 (APOO), Mic27 (APOOL) and Mic60 (Mitofilin) named after a uniform nomenclature [118]. MICOS is also thought to be responsible for maintaining the structure of mitochondria by forming contact sites between the inner (Mic19, Mic25, and Mic60) and outer membranes (SAM50) [119,120]. MICOS plays a role in the open cristae junction of 10 – 50 nm [121,122], controlling the passage of ions, reactive oxygen species and small proteins. In addition to MICOS, the mitochondrial protein fusion OPA1 has been shown to control the diameter of the junctions and to limit the capacity of cytochrome *c* to diffuse across these junctions [123].

The cristae sheets measure less than 100 nm, which makes them impossible to study by conventional fluorescent microscopy techniques. Therefore, the study of cristae structure has been for a long time limited to EM giving only a glimpse of it, in a fixed state. STED microscopy revealed that the spacing between cristae or the number of cristae per mitochondrion depends on the cell type. For adipocyte and neuron mitochondria, the spacing would be 40 - 80 nm, compared with 70 - 150 nm in mitochondria of immortalised cell lines HeLA and COS-7 [81]. Using various SRM techniques and their association with EM, it has been possible to study the MICOS complex and the interaction of its proteins. Stefan Jakobs's team is a pioneer in this field and has made numerous advances. The sufficiency of Mic60 for the formation of crista junctions has been demonstrated [68] and SAM50 would be the anchoring point to guide cristae junction formation [124]. Mic60 forms regular clusters with an opposite distribution in two bands with a twist forming a helix [125,126]. The spatial distribution of Mic60-subcomplexes is thought to be determined antagonistically by OPA1 and Mic10, by extending or restricting their distribution respectively [68]. OPA1 would also be responsible for stabilising cristae junctions and its action with F1F0-ATP synthase would allow the positioning of MICOS at crista junctions [68]. In addition, SRM has recently revealed that Myo19 participates in the stabilisation of crista structure through the SAM-MICOS complexes [127]. Multiple pathologies have been associated with a morphological defect in cristae, highlighting the importance of deciphering their biogenesis. For example mutations in CHCHD10 a protein associated to MICOS complex have been shown to induce MICOS disassembly and to be involved in motor neurone pathologies such as frontotemporal dementia-amyotrophic lateral sclerosis [128].

7. SRM has led to a rethink of mitochondrial bioenergetics with the demonstration of mitochondrial membrane potential (ΔΨm) heterogeneity from cristae to cristae

The ΔΨm is a result of the OXPHOS, created from the balance between the mitochondrial respiratory chain (MRC) activity, which pumps protons at complexes I, III, and IV from the matrix to the inner membrane space (IMS), and the F1F0-ATP synthase, which exploits the resulting proton gradients (Δp) to drive the conversion of ADP to ATP [129]. The ΔΨm is thus essential to several mitochondrial functions (for review see [130]), the import of mitochondrial proteins encoded by the nuclear genome, and the transport of respiratory substrates. For a long time, the ΔΨm was assumed to be homogeneous in a mitochondrion [131,132]. New imaging techniques enabling to monitor the inner compartments of mitochondria, and more specifically live approaches such as ISM microscopy and STED, have made now possible to visualise the cristae of the same mitochondrion separately. It was recently shown, using the fluorescent dye tetramethylrhodamine ethyl ester (TMRE, TMRM) for which mitochondrial accumulation is dependent on ΔΨm, that there is a heterogeneity in ΔΨm between cristae of the same mitochondrion [133]. This difference in ΔΨm could be used as an index of the positioning of the fission actors, as shown by iSIM images of COS-7 cells from the African green monkey and mouse cardiomyocytes, where most mitochondrial fissions that occur at the periphery of the mitochondrial network are preceded by a decrease in ΔΨm [96]. The increase in ΔΨm can also be a critical information, which sometimes is linked to the phenotype of cancer cells [134], exploring cristae ΔΨm heterogeneity by SRM modalities in neurodegenerative or cancer studies will provide essential data for the development of new treatments.

8. SRM has opened up the field of exploration of mitochondrial inner membrane dynamics and cristae remodelling

The development of more and more sensitive photon sensors has led to the improvement of time-lapse imaging and made it possible to reveal the incredible dynamics of organelles, particularly mitochondria, with improved temporal resolution and/or reduced excitation dose. Indeed, it needs to be noted that the excitation of fluorophores leads to the

production of Reactive Oxygen Species (ROS) which may induce the formation of swellings thus altering mitochondrial integrity and can distort the interpretation of mitochondrial exploration. Time-lapse imaging must therefore be acquired with sufficiently high sensitivity and a low excitation dose to reduce the formation of ROS. Recent progresses in labelling strategies and SRM technologies sensitivity have provided impressive new images of mitochondrial dynamics and the inner membrane remodelling. Live-cell SIM, STED and ISM offer now the possibility to decipher the dynamics of mitochondrial cristae. Although previous studies demonstrated that the OXPHOS complexes were at the cristae [135,136], it was not possible to look at the functional significance and dynamism of the inner membrane invaginations. Thanks to live observation using SRM techniques, several teams were able to show that cristae and crista junctions are highly dynamic structures, in opposition to the usual view of static cristae mainly provided by EM. Furthermore, live SRM also demonstrated that leveraging on the non-homogeneous distribution of cristae along the mitochondria, mitochondrial fission takes place at locations with a void in cristae [81]. Besides, it also shown that when two mitochondria fuse, their cristae also fuse, harbouring heterogeneous architecture such as lamellar cristae, arches or interconnected [137]. In addition to mitochondria dynamism during fission/fusion, live SIM shown that cristae are constantly remodelling through elongation, shrinking, fusing and dividing events occurring in few seconds [69,138]. Another team has shown by live STED microscopy that when crista junctions are moving, they are bringing with them the cristae they belong to creating a "V" like structure when two crista junctions are getting closer [139]. Moreover, they observed internal merges between cristae forming "X" or "Y" like structures. Nevertheless, they mentioned that these events are not lasting but are often followed by crista splitting. The development of new SRM approaches which requires increasingly lower light doses (SIM, RESOLFT,…) offers a whole new range of possibilities for the observation of mitochondria dynamics.

As with many other biological objects, real-time imaging of mitochondria raises several challenges in SRM ranging from the photobleaching of the probes, to the relatively low overall temporal resolution of SRM depending on the dynamics to be probed. Another particularly crucial challenge is the phototoxicity of imaging methods that may alter the structures observed over time, rapidly causing mitochondrial swelling. Indeed, mitochondria are highly sensitive to external cues and it has been shown that their membranes depolarise under the effect of lasers, which alters their structure and functions [140]. Yet, SRM typically requires powerful lasers with specific probes or fluorescent markers that are resistant to photobleaching and, at the same time, must be membrane permeable and biocompatible for live observation (for a review of the different classes of marker and specificity for SRM on mitochondria, see [141]). To overcome these emerging challenges, new fluorescent markers are being developed, such as Mito PB Yellow [142], MitoESq-635 [143], which marks the inner membrane of mitochondria but would be more stable over time than other markers, and PK mito orange (PKMO), which also promises to be more stable and has the advantage to be compatible with other markers for multi-colour live-cell imaging [81]. More recently, a novel class of fluorescent probes have been highlighted, amphiphilic aggregation-induced emission with AC-QC nanoparticles, which can be used to study mitochondria in live-cell. The advantage of this new probe would be a lower cytotoxicity, a higher photostability enabling longer and/or faster acquisition in live-cell [144].

9. SRM has been successfully used to visualise the pores on the surface of mitochondria that form during apoptotic induction

Apoptosis is the programmed cell death, divided in two pathways: the extrinsic pathway drove by the activation of death receptors by stimuli coming from the environment, and the intrinsic pathway drove by internal stimuli in which mitochondria have a crucial role [145]. In response to a noxious stimulus (e.g. DNA damage, cytotoxic stress,.) [146,147], the mitochondrial outer membrane creates large pore through the process called Mitochondrial Outer Membrane Permeabilization (MOMP) (Fig. 2). It leads to the release of pro-apoptotic signals (such as cytochrome *c*) in the cytosol and the activation of caspase, which results in apoptosis. BAX and BAK, two proteins from the BCL-2 family [148] are required for the MOMP [149,150]. At a basal state, BAX is mainly located in the cytosol and is translocated to the mitochondrial outer membrane upon apoptosis activation to oligomerise and create MOMP. Whereas BAK is already, mainly located at the mitochondrial outer membrane. Defects in apoptotic mechanisms are implicated in multiples pathologies including cancer and neurodegenerative disorders [151,152], making their understanding even more important to developed new treatment [153].

In the last decade SRM has provided new details in apoptosis and MOMP mechanisms that could not be observed by conventional microscopy and complete the past knowledge. In 2016, at the same time two teams showed upon apoptosis activation, by STED microscopy and SMLM, the accumulation of BAX into large clusters in line, arc, or ring structures with the two last ones able to create MOMP [154,155]. Furthermore, it has previously been shown that mitochondria can trigger apoptosis in a caspase-independent mechanism by realising mtDNA into the cytosol (Fig. 2). Thus, an inflammatory response is initiated through the cyclic GMP-AMP synthase/stimulator of interferon genes (cGAS/STING) signalling pathway leading to the secretion of type I interferon [156,157]. However, it was unclear how mitochondria could release mtDNA until SRM visualised the formation of macropores by BAX and BAK allowing the mitochondrial inner membrane to be extruded into the cytosol, carrying matrix component including mtDNA [158,159]. More recently, another team studied the BAX/BAK organisation by SRM showing that as previously demonstrated for BAX, BAK also aggregates into heterogeneous line, arc and ring structures [160]. Nevertheless, BAK clusters are smaller, more homogeneous in size, and form more quickly than BAX oligomers. BAK can also recruits BAX to form together a supra-molecular apoptotic structure. BAK/BAX regulate each other's assembly and the dynamic of pore growth leading to a fine-tuned of the inflammatory outcome of apoptosis.

10. SRM has provided data on the biophysics of membranes in the mitochondria of living cells

Mitochondrial dynamics is essential for shaping the mitochondrial network, maintaining a healthy mitochondrial population, and enabling metabolic adaptations. Nevertheless, we are less aware that lipids and proteins in the mitochondrial membranes also have dynamics in terms of lateral mobility and translocation. These single-molecule dynamics are equally important for the above processes, as they allow interaction with other proteins and complexes. Improved sptPALM technologies in live-cells, using brighter organic dyes in place of conventional photoactivable fluorescent proteins [161,162], provide nanoscopic localisation and mobility maps of mitochondrial proteins *in situ*. It makes it possible to study the specific spatiotemporal organisation of proteins and lipids in relation to mitochondrial function and adaptation. Which respiratory proteins are preferentially localised in the crista sheets or on the peripheral inner membranes, and what are the dynamics of the MICOS complex? The bioenergetic activity of mitochondria, to mention just one, varies continuously according to the metabolic needs of the cell. The organisation of the proteins into complexes therefore adapts accordingly, even moving from one membrane to another. Trajectory models show the limits to their mobility and how this determines their distribution. We are at the beginning of quantifying their diffusion constants in the respective membranes, which will allow to study the formation of super-complexes. The technique is based on the use of brighter organic photostable fluorophore attached specifically to HaloTag7® protein [161] or SNAP-tagged proteins in mitochondrial membranes [80]. Single particle tracking yields individual trajectories

that can be further analysed in terms of directionality. The trajectories of different mitochondrial proteins depend on the organisation of the mitochondria, thus for inner membrane proteins it is expected that they will show preferentially a longitudinal movement. The longitudinal axis, 500 – 800 nm long on average, is longer than the perpendicular axis of the mitochondria which is determined by the diameter of the tubular organelles. On the other hand, proteins localised at the cristae (such as OXPHOS proteins) will predominantly have an orthogonal movement. Still confined to a limited number of teams, sptPALM will provide a major insight into mitochondrial membrane dynamics. These data have confirmed the presence of a broad matrix continuum allowing diffusion of the components inside the mitochondria. SptPALM has also shown that the diffusion rates are much higher than previously shown, with rates of less than 0.2 μm^2/sec [163]. Depending on the protein's location in the mitochondria, the value of the diffusion coefficients calculated from the mean square displacements of the individual molecules can vary from 0.070 μm^2/s in the outer membrane [164], to 0.018 μm^2/s in inner membrane. The rapidity of these events may require an acquisition capacity of 100 Hz [63], potentially out of reach of conventional sptPALM approaches but in the scope of the new MINFLUX technique (Table 1).

11. SRM changes our perception of mitochondrial imaging

Observing the nanoscale organisation of key actors in the mitochondria in relation to the mitochondrial membrane and mitochondria compartments would provide a better understanding of the structure-function relationship in mitochondria.

However, the achievable resolution of SRM, and especially of SMLM or MINFLUX, has raised new challenges such as the accurate and efficient labelling of the observed structure, as well as the effective detection of each fluorophore. Indeed, achieving molecular scale resolution in SMLM [165] or in MINFLUX, raises the question of the distance between the fluorescent label and the protein of interest, which lead to an inaccurate localisation of the protein of interest itself. New tag and labelling approaches are and need to be developed to reduce this distance from the use of nanobodies, affinity tags, or small molecule binders up to the development of unnatural amino acids bound to organic fluorophore [166].

As pointing accuracy increases, it also becomes increasingly difficult to locate enough individual molecules to be able to faithfully reconstruct a complex structure with all its fine details. In conventional approaches, it may lead to very long acquisition time incompatible with routine use. Furthermore, conventional localisation algorithm usually failed to accurately localise single molecule when they are too dense, especially in 3D [167]. Recently deep-learning based approaches have allowed to increase the density of single molecules that can be located per frames, thus considerably reducing the total acquisition time by an order of magnitude or more for the same number of final locations [168,169]. Those approaches have led to important breakthrough in SRM imaging, greatly reducing acquisition time and increasing imaging throughput for more systematic studies. Combined with automated imaging methods it may provide an interesting tool for the identification and study of mitochondria key players [170].

12. Concluding remarks and outlook

SRM technologies continue to progress thanks to advances in optics, cameras, and computing sciences. Similarly, chemists and biologists are developing remarkable tools to label mitochondrial targets more closely, as well as to target endogenous partners to approach physiological conditions. Recent advances have been made with dyes based on luminescent transition metal complexes, which enable mitochondrial dynamics to be effectively monitored under SIM [171] and SRM has also benefited from the strong development of fluorescent lipid probes (and vice versa), providing markers for studying lipid nanodomains, the composition of mitochondrial membranes, and traffic between mitochondrial compartments and other cellular organelles.

Thus, SRM is already providing new biological data to clarify and to improve our understanding of mitochondrial physiological and pathophysiological mechanisms. The possibility of using radiometric probes in SRM will allow the quantification of mitochondrial micro-nano events as the $\Delta\Psi m$ drop in a crista, the ability to monitor micro, nano, and mitophagy events [172] and to monitor different calcium ion concentrations and their location [173].

As we have tried to explain, SRM imaging makes it possible for the first time to obtain biophysical data, usually from acellular systems or isolated mitochondria within living cells. In this development, SRM measurements will be particularly interesting to study some concepts such as the temperature of mitochondria [174–177], or the distribution and utilisation of ATP pools [178].

As you can read in recent publications and reviews, these new SRM data and the mapping of proteins within mitochondrial networks requires new image analysis tools to enable analyses such as segmentation, clustering, tracking or co-location [179–181]. Automating SRM acquisitions and using artificial intelligence to analyse data will speed up quantification and extract new cross-referenced data. A first publication already showed that trainable segmentation machine-learning tool enables cristae quantification in a way that is unbiased by human analysis [137].

In short, the mitochondria, due to the complexity of its structure and the richness of its metabolic activities, are super-organelles that challenge the possibilities of super-resolution imaging, allowing biologists to progressively access observations that were unthinkable a few years ago. These advances will make it possible to propose new research strategies, to contribute to a better understanding of the pathophysiological consequences of dynamic mitochondrial genes in rare diseases or to refine nanoscopic observations of mitochondrial defects in common pathologies such as cancer or Parkinson's/Alzheimer's disease.

Funding

This research was funded by grants from the University of Angers, CNRS, and INSERM.

Declaration of Competing Interest

The authors declare that they have no known competing financial interests or personal relationships that could have appeared to influence the work reported in this paper.

Acknowledgements

This work is supported by funding from the Agence National de la Recherche grant number ANR-21-CE44-0019.

References

[1] S. Cogliati, C. Frezza, M.E. Soriano, T. Varanita, R. Quintana-Cabrera, M. Corrado, et al., Mitochondrial cristae shape determines respiratory chain supercomplexes assembly and respiratory efficiency, Cell 155 (2013) 160–171, https://doi.org/10.1016/j.cell.2013.08.032.

[2] A. Mühleip, R.K. Flygaard, R. Baradaran, O. Haapanen, T. Gruhl, V. Tobiasson, et al., Structural basis of mitochondrial membrane bending by the I–II–III2–IV2 supercomplex, Nature 615 (2023) 934–938, https://doi.org/10.1038/s41586-023-05817-y.

[3] K.M. Davies, C. Anselmi, I. Wittig, J.D. Faraldo-Gómez, W. Kühlbrandt, Structure of the yeast F_1F_o-ATP synthase dimer and its role in shaping the mitochondrial cristae, Proc. Natl. Acad. Sci. USA 109 (2012) 13602–13607, https://doi.org/10.1073/pnas.1204593109.

[4] J. He, H.C. Ford, J. Carroll, C. Douglas, E. Gonzales, S. Ding, et al., Assembly of the membrane domain of ATP synthase in human mitochondria, Proc. Natl. Acad. Sci. USA 115 (2018) 2988–2993, https://doi.org/10.1073/pnas.1722086115.

[5] T.B. Blum, A. Hahn, T. Meier, K.M. Davies, W. Kühlbrandt, Dimers of mitochondrial ATP synthase induce membrane curvature and self-assemble into

rows, Proc. Natl. Acad. Sci. USA 116 (2019) 4250–4255, https://doi.org/10.1073/pnas.1816556116.
[6] J.W. Lee, Protonic capacitor: elucidating the biological significance of mitochondrial cristae formation, Sci. Rep. 10 (2020) 10304, https://doi.org/10.1038/s41598-020-66203-6.
[7] A.J. Roger, S.A. Muñoz-Gómez, R. Kamikawa, The origin and diversification of mitochondria, Curr. Biol. 27 (2017) R1177–R1192, https://doi.org/10.1016/j.cub.2017.09.015.
[8] R.W. Gilkerson, D.H. Margineantu, R.A. Capaldi, J.M.L. Selker, Mitochondrial DNA depletion causes morphological changes in the mitochondrial reticulum of cultured human cells, FEBS Lett. 474 (2000) 1–4, https://doi.org/10.1016/S0014-5793(00)01527-1.
[9] N. Ikon, R.O. Ryan, Cardiolipin and mitochondrial cristae organization, Biochim. Biophys. Acta Biomembr. 1859 (2017) 1156–1163, https://doi.org/10.1016/j.bbamem.2017.03.013.
[10] F. Pelliccione, A. Micillo, G. Cordeschi, A. D'Angeli, S. Necozione, L. Gandini, et al., Altered ultrastructure of mitochondrial membranes is strongly associated with unexplained asthenozoospermia, Fertil. Steril. 95 (2011) 641–646, https://doi.org/10.1016/j.fertnstert.2010.07.1086.
[11] M. Picard, K. White, D.M. Turnbull, Mitochondrial morphology, topology, and membrane interactions in skeletal muscle: a quantitative three-dimensional electron microscopy study, J. Appl. Physiol. 114 (2013) 161–171, https://doi.org/10.1152/japplphysiol.01096.2012.
[12] M. Picard, M.J. McManus, G. Csordás, P. Várnai, G.W. Dorn II, D. Williams, et al., Trans-mitochondrial coordination of cristae at regulated membrane junctions, Nat. Commun. 6 (2015) 6259, https://doi.org/10.1038/ncomms7259.
[13] A.E. Vincent, Y.S. Ng, K. White, T. Davey, C. Mannella, G. Falkous, et al., The spectrum of mitochondrial ultrastructural defects in mitochondrial myopathy, Sci. Rep. 6 (2016) 30610, https://doi.org/10.1038/srep30610.
[14] B.N.G. Giepmans, S.R. Adams, M.H. Ellisman, R.Y. Tsien, The fluorescent toolbox for assessing protein location and function, Science 312 (2006) 217–224, https://doi.org/10.1126/science.1124618.
[15] F. Malka, O. Guillery, C. Cifuentes-Diaz, E. Guillou, P. Belenguer, A. Lombès, et al., Separate fusion of outer and inner mitochondrial membranes, EMBO Rep. 6 (2005) 853–859, https://doi.org/10.1038/sj.embor.7400488.
[16] T.S. Fung, R. Chakrabarti, H.N. Higgs, The multiple links between actin and mitochondria, Nat. Rev. Mol. Cell Biol. (2023), https://doi.org/10.1038/s41580-023-00613-y.
[17] J. Bereiter-Hahn, M. Vöth, Dynamics of mitochondria in living cells: shape changes, dislocations, fusion, and fission of mitochondria, Microsc. Res Tech. 27 (1994) 198–219, https://doi.org/10.1002/jemt.1070270303.
[18] E.P. Bulthuis, M.J.W. Adjobo-Hermans, P.H.G.M. Willems, W.J.H. Koopman, Mitochondrial Morphofunction in Mammalian Cells, Antioxid. Redox Signal. 30 (2019) 2066–2109, https://doi.org/10.1089/ars.2018.7534.
[19] Z. Song, M. Ghochani, J.M. McCaffery, T.G. Frey, D.C. Chan, Mitofusins and OPA1 mediate sequential steps in mitochondrial membrane fusion, MBoC 20 (2009) 3525–3532, https://doi.org/10.1091/mbc.e09-03-0252.
[20] S. Gao, J. Hu, Mitochondrial fusion: the machineries in and out, Trends Cell Biol. 31 (2021) 62–74, https://doi.org/10.1016/j.tcb.2020.09.008.
[21] O.M. de Brito, L. Scorrano, Mitofusin 2 tethers endoplasmic reticulum to mitochondria, Nature 456 (2008) 605–610, https://doi.org/10.1038/nature07534.
[22] T.D. Fischer, P.K. Dash, J. Liu, M.N. Waxham, Morphology of mitochondria in spatially restricted axons revealed by cryo-electron tomography, PLoS Biol. 16 (2018) e2006169, https://doi.org/10.1371/journal.pbio.2006169.
[23] Y.M. Sigal, R. Zhou, X. Zhuang, Visualizing and discovering cellular structures with super-resolution microscopy, Science 361 (2018) 880–887, https://doi.org/10.1126/science.aau1044.
[24] A. Szymborska, A. de Marco, N. Daigle, V.C. Cordes, J.A.G. Briggs, J. Ellenberg, Nuclear pore scaffold structure analyzed by super-resolution microscopy and particle averaging, Science 341 (2013) 655–658, https://doi.org/10.1126/science.1240672.
[25] H.Y. Suleiman, R. Roth, S. Jain, J.E. Heuser, A.S. Shaw, J.H. Miner, Injury-induced actin cytoskeleton reorganization in podocytes revealed by super-resolution microscopy, JCI Insight 2 (2017) e94137, https://doi.org/10.1172/jci.insight.94137.
[26] K. Xu, G. Zhong, X. Zhuang, Actin, spectrin, and associated proteins form a periodic cytoskeletal structure in axons, Science 339 (2013) 452–456, https://doi.org/10.1126/science.1232251.
[27] J. Xu, Y. Liu, Probing chromatin compaction and its epigenetic states in situ with single-molecule localization-based super-resolution microscopy, Front Cell Dev. Biol. 9 (2021) 653077, https://doi.org/10.3389/fcell.2021.653077.
[28] H. Wang, G. Fang, H. Chen, M. Hu, Y. Cui, B. Wang, et al., Lysosome-targeted biosensor for the super-resolution imaging of lysosome–mitochondrion interaction, Front Pharm. 13 (2022) 865173, https://doi.org/10.3389/fphar.2022.865173.
[29] Y. Guo, D. Li, S. Zhang, Y. Yang, J.-J. Liu, X. Wang, et al., Visualizing intracellular organelle and cytoskeletal interactions at nanoscale resolution on millisecond timescales, 1430-1442.e17, Cell 175 (2018), https://doi.org/10.1016/j.cell.2018.09.057.
[30] D. Hanahan, R.A. Weinberg, Hallmarks of cancer: the next generation, Cell 144 (2011) 646–674, https://doi.org/10.1016/j.cell.2011.02.013.
[31] M. Han, E.A. Bushong, M. Segawa, A. Tiard, A. Wong, M.R. Brady, et al., Spatial mapping of mitochondrial networks and bioenergetics in lung cancer, Nature 615 (2023) 712–719, https://doi.org/10.1038/s41586-023-05793-3.
[32] Z. Al Amir Dache, A.R. Thierry, Mitochondria-derived cell-to-cell communication, Cell Rep. 42 (2023) 112728, https://doi.org/10.1016/j.celrep.2023.112728.
[33] B.P. Rickard, M. Overchuk, V.A. Chappell, M. Kemal Ruhi, P.D. Sinawang, T. T. Nguyen Hoang, et al., Methods to evaluate changes in mitochondrial structure and function in cancer, Cancers 15 (2023) 2564, https://doi.org/10.3390/cancers15092564.
[34] E. Abbe, Beiträge zur theorie des mikroskops und der mikroskopischen wahrnehmung, Arch. F. Mikros Anat. 9 (1873) 413–468, https://doi.org/10.1007/BF02956173.
[35] M.G.L. Gustafsson, Surpassing the lateral resolution limit by a factor of two using structured illumination microscopy, J. Microsc. 198 (2000) 82–87, https://doi.org/10.1046/j.1365-2818.2000.00710.x.
[36] M.G.L. Gustafsson, Nonlinear structured-illumination microscopy: wide-field fluorescence imaging with theoretically unlimited resolution, Proc. Natl. Acad. Sci. USA 102 (2005) 13081–13086, https://doi.org/10.1073/pnas.0406877102.
[37] S.W. Hell, J. Wichmann, Breaking the diffraction resolution limit by stimulated emission: stimulated-emission-depletion fluorescence microscopy, Opt. Lett. 19 (1994) 780, https://doi.org/10.1364/OL.19.000780.
[38] T.A. Klar, S. Jakobs, M. Dyba, A. Egner, S.W. Hell, Fluorescence microscopy with diffraction resolution barrier broken by stimulated emission, Proc. Natl. Acad. Sci. USA 97 (2000) 8206–8210, https://doi.org/10.1073/pnas.97.15.8206.
[39] F. Balzarotti, Y. Eilers, K.C. Gwosch, A.H. Gynnå, V. Westphal, F.D. Stefani, et al., Nanometer resolution imaging and tracking of fluorescent molecules with minimal photon fluxes, Science 355 (2017) 606–612, https://doi.org/10.1126/science.aak9913.
[40] S.W. Hell, Far-field optical nanoscopy, Science 316 (2007) 1153–1158, https://doi.org/10.1126/science.1137395.
[41] Y. Hirano, A. Matsuda, Y. Hiraoka, Recent advancements in structured-illumination microscopy toward live-cell imaging, Microscopy 64 (2015) 237–249, https://doi.org/10.1093/jmicro/dfv034.
[42] M.G.L. Gustafsson, L. Shao, P.M. Carlton, C.J.R. Wang, I.N. Golubovskaya, W. Z. Cande, et al., Three-dimensional resolution doubling in wide-field fluorescence microscopy by structured illumination, Biophys. J. 94 (2008) 4957–4970, https://doi.org/10.1529/biophysj.107.120345.
[43] Y. Wu, H. Shroff, Faster, sharper, and deeper: structured illumination microscopy for biological imaging, Nat. Methods 15 (2018) 1011–1019, https://doi.org/10.1038/s41592-018-0211-z.
[44] N. Kilian, A. Goryaynov, M.D. Lessard, G. Hooker, D. Toomre, J.E. Rothman, et al., Assessing photodamage in live-cell STED microscopy, Nat. Methods 15 (2018) 755–756, https://doi.org/10.1038/s41592-018-0145-5.
[45] M. Hofmann, C. Eggeling, S. Jakobs, S.W. Hell, Breaking the diffraction barrier in fluorescence microscopy at low light intensities by using reversibly photoswitchable proteins, Proc. Natl. Acad. Sci. USA 102 (2005) 17565–17569, https://doi.org/10.1073/pnas.0506010102.
[46] A. Chmyrov, J. Keller, T. Grotjohann, M. Ratz, E. d'Este, S. Jakobs, et al., Nanoscopy with more than 100,000 "doughnuts", Nat. Methods 10 (2013) 737–740, https://doi.org/10.1038/nmeth.2556.
[47] L.A. Masullo, A. Bodén, F. Pennacchietti, G. Coceano, M. Ratz, I. Testa, Enhanced photon collection enables four dimensional fluorescence nanoscopy of living systems, Nat. Commun. 9 (2018) 3281, https://doi.org/10.1038/s41467-018-05799-w.
[48] A. Bodén, F. Pennacchietti, G. Coceano, M. Damenti, M. Ratz, I. Testa, Volumetric live cell imaging with three-dimensional parallelized RESOLFT microscopy, Nat. Biotechnol. 39 (2021) 609–618, https://doi.org/10.1038/s41587-020-00779-2.
[49] V. Ebrahimi, T. Stephan, J. Kim, P. Carravilla, C. Eggeling, S. Jakobs, et al., Deep learning enables fast, gentle STED microscopy, Commun. Biol. 6 (2023) 674, https://doi.org/10.1038/s42003-023-05054-z.
[50] M. Lelek, M.T. Gyparaki, G. Beliu, F. Schueder, J. Griffié, S. Manley, et al., Single-molecule localization microscopy, Nat. Rev. Methods Prim. 1 (2021) 39, https://doi.org/10.1038/s43586-021-00038-x.
[51] H. Deschout, F.C. Zanacchi, M. Mlodzianoski, A. Diaspro, J. Bewersdorf, S. T. Hess, et al., Precisely and accurately localizing single emitters in fluorescence microscopy, Nat. Methods 11 (2014) 253–266, https://doi.org/10.1038/nmeth.2843.
[52] E. Betzig, G.H. Patterson, R. Sougrat, O.W. Lindwasser, S. Olenych, J. S. Bonifacino, et al., Imaging intracellular fluorescent proteins at nanometer resolution, Science 313 (2006) 1642–1645, https://doi.org/10.1126/science.1127344.
[53] S.T. Hess, T.P.K. Girirajan, M.D. Mason, Ultra-high resolution imaging by fluorescence photoactivation localization microscopy, Biophys. J. 91 (2006) 4258–4272, https://doi.org/10.1529/biophysj.106.091116.
[54] M.J. Rust, M. Bates, X. Zhuang, Sub-diffraction-limit imaging by stochastic optical reconstruction microscopy (STORM), Nat. Methods 3 (2006) 793–796, https://doi.org/10.1038/nmeth929.
[55] M. Heilemann, S. vandeLinde, M. Schüttpelz, R. Kasper, B. Seefeldt, A. Mukherjee, et al., Subdiffraction-resolution fluorescence imaging with conventional fluorescent probes, Angew. Chem. Int Ed. 47 (2008) 6172–6176, https://doi.org/10.1002/anie.200802376.
[56] G. Giannone, E. Hosy, F. Levet, A. Constals, K. Schulze, A.I. Sobolevsky, et al., Dynamic superresolution imaging of endogenous proteins on living cells at ultra-high density, Biophys. J. 99 (2010) 1303–1310, https://doi.org/10.1016/j.bpj.2010.06.005.
[57] R. Jungmann, C. Steinhauer, M. Scheible, A. Kuzyk, P. Tinnefeld, F.C. Simmel, Single-molecule kinetics and super-resolution microscopy by fluorescence imaging of transient binding on DNA origami, Nano Lett. 10 (2010) 4756–4761, https://doi.org/10.1021/nl103427w.

[58] A. Sharonov, R.M. Hochstrasser, Wide-field subdiffraction imaging by accumulated binding of diffusing probes, Proc. Natl. Acad. Sci. USA 103 (2006) 18911–18916, https://doi.org/10.1073/pnas.0609643104.
[59] S. Manley, J.M. Gillette, G.H. Patterson, H. Shroff, H.F. Hess, E. Betzig, et al., High-density mapping of single-molecule trajectories with photoactivated localization microscopy, Nat. Methods 5 (2008) 155–157, https://doi.org/10.1038/nmeth.1176.
[60] T.A. Brown, A.N. Tkachuk, G. Shtengel, B.G. Kopek, D.F. Bogenhagen, H.F. Hess, et al., Superresolution fluorescence imaging of mitochondrial nucleoids reveals their spatial range, limits, and membrane interaction, Mol. Cell. Biol. 31 (2011) 4994–5010, https://doi.org/10.1128/MCB.05694-11.
[61] K.C. Gwosch, J.K. Pape, F. Balzarotti, P. Hoess, J. Ellenberg, J. Ries, et al., MINFLUX nanoscopy delivers 3D multicolor nanometer resolution in cells, Nat. Methods 17 (2020) 217–224, https://doi.org/10.1038/s41592-019-0688-0.
[62] T. Deguchi, M.K. Iwanski, E.-M. Schentarra, C. Heidebrecht, L. Schmidt, J. Heck, et al., Direct observation of motor protein stepping in living cells using MINFLUX, Science 379 (2023) 1010–1015, https://doi.org/10.1126/science.ade2676.
[63] K.B. Busch, Inner mitochondrial membrane compartmentalization: dynamics across scales, Int. J. Biochem. Cell Biol. 120 (2020) 105694, https://doi.org/10.1016/j.biocel.2020.105694.
[64] M. Tokunaga, N. Imamoto, K. Sakata-sogawa, Highly inclined thin illumination enables clear single-molecule imaging in cells, Nat. Methods 5 (2008) 159–161, https://doi.org/10.1038/NMETH.1171.
[65] B.-C. Chen, W.R. Legant, K. Wang, L. Shao, D.E. Milkie, M.W. Davidson, et al., Lattice light-sheet microscopy: imaging molecules to embryos at high spatiotemporal resolution, Science 346 (2014) 1257998, https://doi.org/10.1126/science.1257998.
[66] R. Galland, G. Grenci, A. Aravind, V. Viasnoff, V. Studer, J.-B. Sibarita, 3D high- and super-resolution imaging using single-objective SPIM, Nat. Methods 12 (2015) 641–644, https://doi.org/10.1038/nmeth.3402.
[67] A.-K. Gustavsson, P.N. Petrov, M.Y. Lee, Y. Shechtman, W.E. Moerner, 3D single-molecule super-resolution microscopy with a tilted light sheet, Nat. Commun. 9 (2018) 123, https://doi.org/10.1038/s41467-017-02563-4.
[68] T. Stephan, C. Brüser, M. Deckers, A.M. Steyer, F. Balzarotti, M. Barbot, et al., MICOS assembly controls mitochondrial inner membrane remodeling and crista junction redistribution to mediate cristae formation, EMBO J. 39 (2020) e104105, https://doi.org/10.15252/embj.2019104105.
[69] X. Huang, J. Fan, L. Li, H. Liu, R. Wu, Y. Wu, et al., Fast, long-term, super-resolution imaging with Hessian structured illumination microscopy, Nat. Biotechnol. 36 (2018) 451–459, https://doi.org/10.1038/nbt.4115.
[70] G. Donnert, J. Keller, C.A. Wurm, S.O. Rizzoli, V. Westphal, A. Schönle, et al., Two-color far-field fluorescence nanoscopy, Biophys. J. 92 (2007) L67–L69, https://doi.org/10.1529/biophysj.107.104497.
[71] M.J. Young, W.C. Copeland, Human mitochondrial DNA replication machinery and disease, Curr. Opin. Genet. Dev. 38 (2016) 52–62, https://doi.org/10.1016/j.gde.2016.03.005.
[72] G. Monzio Compagnoni, A. Di Fonzo, S. Corti, G.P. Comi, N. Bresolin, E. Masliah, The role of mitochondria in neurodegenerative diseases: the lesson from alzheimer's disease and parkinson's disease, Mol. Neurobiol. 57 (2020) 2959–2980, https://doi.org/10.1007/s12035-020-01926-1.
[73] P. Bottoni, G. Gionta, R. Scatena, Remarks on mitochondrial myopathies, IJMS 24 (2022) 124, https://doi.org/10.3390/ijms24010124.
[74] F. Legros, F. Malka, P. Frachon, A. Lombès, M. Rojo, Organization and dynamics of human mitochondrial DNA, J. Cell Sci. 117 (2004) 2653–2662, https://doi.org/10.1242/jcs.01134.
[75] E. Ylikallio, H. Tyynismaa, H. Tsutsui, T. Ide, A. Suomalainen, High mitochondrial DNA copy number has detrimental effects in mice, Hum. Mol. Genet. 19 (2010) 2695–2705, https://doi.org/10.1093/hmg/ddq163.
[76] C. Kukat, C.A. Wurm, H. Spahr, M. Falkenberg, N.-G. Larsson, S. Jakobs, Super-resolution microscopy reveals that mammalian mitochondrial nucleoids have a uniform size and frequently contain a single copy of mtDNA, Proc. Natl. Acad. Sci. 108 (2011) 13534–13539, https://doi.org/10.1073/pnas.1109263108.
[77] C. Kukat, K.M. Davies, C.A. Wurm, H. Spåhr, N.A. Bonekamp, I. Kühl, et al., Cross-strand binding of TFAM to a single mtDNA molecule forms the mitochondrial nucleoid, Proc. Natl. Acad. Sci. USA 112 (2015) 11288–11293, https://doi.org/10.1073/pnas.1512131112.
[78] V. Pavluch, T. Špaček, H. Engstová, A. Dlasková, P. Ježek, Possible frequent multiple mitochondrial DNA copies in a single nucleoid in HeLa cells, Sci. Rep. 13 (2023) 5788, https://doi.org/10.1038/s41598-023-33012-6.
[79] B.G. Kopek, G. Shtengel, C.S. Xu, D.A. Clayton, H.F. Hess, Correlative 3D superresolution fluorescence and electron microscopy reveal the relationship of mitochondrial nucleoids to membranes, Proc. Natl. Acad. Sci. 109 (2012) 6136–6141, https://doi.org/10.1073/pnas.1121558109.
[80] T. Stephan, A. Roesch, D. Riedel, S. Jakobs, Live-cell STED nanoscopy of mitochondrial cristae, Sci. Rep. 9 (2019) 12419, https://doi.org/10.1038/s41598-019-48838-2.
[81] T. Liu, T. Stephan, P. Chen, J. Keller-Findeisen, J. Chen, D. Riedel, et al., Multi-color live-cell STED nanoscopy of mitochondria with a gentle inner membrane stain, Proc. Natl. Acad. Sci. USA 119 (2022) e2215799119, https://doi.org/10.1073/pnas.2215799119.
[82] M. Feric, T.G. Demarest, J. Tian, D.L. Croteau, V.A. Bohr, T. Misteli, Self-assembly of multi-component mitochondrial nucleoids via phase separation, EMBO J. 40 (2021) e107165, https://doi.org/10.15252/embj.2020107165.
[83] Q. Long, Y. Zhou, H. Wu, S. Du, M. Hu, J. Qi, et al., Phase separation drives the self-assembly of mitochondrial nucleoids for transcriptional modulation, Nat. Struct. Mol. Biol. 28 (2021) 900–908, https://doi.org/10.1038/s41594-021-00671-w.
[84] J. Qin, Y. Guo, B. Xue, P. Shi, Y. Chen, Q.P. Su, et al., ER-mitochondria contacts promote mtDNA nucleoids active transportation via mitochondrial dynamic tubulation, Nat. Commun. 11 (2020) 4471, https://doi.org/10.1038/s41467-020-18202-4.
[85] F. Kraus, K. Roy, T.J. Pucadyil, M.T. Ryan, Function and regulation of the divisome for mitochondrial fission, Nature 590 (2021) 57–66, https://doi.org/10.1038/s41586-021-03214-x.
[86] H. Tamada, S. Kiryu-Seo, H. Hosokawa, K. Ohta, N. Ishihara, M. Nomura, et al., Three-dimensional analysis of somatic mitochondrial dynamics in fission-deficient injured motor neurons using FIB/SEM, J. Comp. Neurol. 525 (2017) 2535–2548, https://doi.org/10.1002/cne.24213.
[87] D. Loiseau, A. Chevrollier, C. Verny, V. Guillet, N. Gueguen, M.-A. Pou De Crescenzo, et al., Mitochondrial coupling defect in Charcot-Marie-Tooth type 2A disease, Ann. Neurol. 61 (2007) 315–323, https://doi.org/10.1002/ana.21086.
[88] A.B. Knott, G. Perkins, R. Schwarzenbacher, E. Bossy-Wetzel, Mitochondrial fragmentation in neurodegeneration, Nat. Rev. Neurosci. 9 (2008) 505–518, https://doi.org/10.1038/nrn2417.
[89] Chevrollier A., Alice Bonnard A., Ruaud L., Gueguen N., Perrin L., Desquiret-Dumas V., et al. Homozygous MFN2 variants causing severe antenatal encephalopathy with clumped mitochondria. Brain in press.
[90] N.M.B. Yapa, V. Lisnyak, B. Reljic, M.T. Ryan, Mitochondrial dynamics in health and disease, FEBS Lett. 595 (2021) 1184–1204, https://doi.org/10.1002/1873-3468.14077.
[91] W. Ji, A.L. Hatch, R.A. Merrill, S. Strack, H.N. Higgs, Actin filaments target the oligomeric maturation of the dynamin GTPase Drp1 to mitochondrial fission sites, ELife 4 (2015) e11553, https://doi.org/10.7554/eLife.11553.
[92] H. Otera, C. Wang, M.M. Cleland, K. Setoguchi, S. Yokota, R.J. Youle, et al., Mff is an essential factor for mitochondrial recruitment of Drp1 during mitochondrial fission in mammalian cells, J. Cell Biol. 191 (2010) 1141–1158, https://doi.org/10.1083/jcb.201007152.
[93] Y. Shi, L. Wang, J. Zhang, Y. Zhai, F. Sun, Determining the target protein localization in 3D using the combination of FIB-SEM and APEX2, Biophys. Rep. 3 (2017) 92–99, https://doi.org/10.1007/s41048-017-0043-x.
[94] C.A. Francy, F.J.D. Alvarez, L. Zhou, R. Ramachandran, J.A. Mears, The mechanoenzymatic core of dynamin-related protein 1 comprises the minimal machinery required for membrane constriction, J. Biol. Chem. 290 (2015) 11692–11703, https://doi.org/10.1074/jbc.M114.610881.
[95] Q. Chen, L.-Y. Liu, Z. Tian, Z. Fang, K.-N. Wang, X. Shao, et al., Mitochondrial nucleoid condensates drive peripheral fission through high membrane curvature, Cell Rep. 42 (2023) 113472, https://doi.org/10.1016/j.celrep.2023.113472.
[96] T. Kleele, T. Rey, J. Winter, S. Zaganelli, D. Mahecic, H. Perreten Lambert, et al., Distinct fission signatures predict mitochondrial degradation or biogenesis, Nature 593 (2021) 435–439, https://doi.org/10.1038/s41586-021-03510-6.
[97] S.M. Coscia, C.P. Thompson, Q. Tang, E.E. Baltrusaitis, J.A. Rhodenhiser, O. A. Quintero-Carmona, et al., Myo19 tethers mitochondria to endoplasmic reticulum-associated actin to promote mitochondrial fission, J. Cell Sci. 136 (2023) jcs260612, https://doi.org/10.1242/jcs.260612.
[98] Y.C. Wong, D. Ysselstein, D. Krainc, Mitochondria–lysosome contacts regulate mitochondrial fission via RAB7 GTP hydrolysis, Nature 554 (2018) 382–386, https://doi.org/10.1038/nature25486.
[99] M. Boutry, P.K. Kim, ORP1L mediated PI(4)P signaling at ER-lysosome-mitochondrion three-way contact contributes to mitochondrial division, Nat. Commun. 12 (2021) 5354, https://doi.org/10.1038/s41467-021-25621-4.
[100] G. Csordás, C. Renken, P. Várnai, L. Walter, D. Weaver, K.F. Buttle, et al., Structural and functional features and significance of the physical linkage between ER and mitochondria, J. Cell Biol. 174 (2006) 915–921, https://doi.org/10.1083/jcb.200604016.
[101] J.R. Friedman, L.L. Lackner, M. West, J.R. DiBenedetto, J. Nunnari, G.K. Voeltz, ER tubules mark sites of mitochondrial division, Science 334 (2011) 358–362, https://doi.org/10.1126/science.1207385.
[102] G. Csordás, P. Várnai, T. Golenár, S. Roy, G. Purkins, T.G. Schneider, et al., Imaging interorganelle contacts and local calcium dynamics at the ER-mitochondrial interface, Mol. Cell 39 (2010) 121–132, https://doi.org/10.1016/j.molcel.2010.06.029.
[103] R. Iwasawa, A.-L. Mahul-Mellier, C. Datler, E. Pazarentzos, S. Grimm, Fis1 and Bap31 bridge the mitochondria-ER interface to establish a platform for apoptosis induction: Fis1 induces apoptosis via Bap31, EMBO J. 30 (2011) 556–568, https://doi.org/10.1038/emboj.2010.346.
[104] J.E. Vance, Phospholipid synthesis in a membrane fraction associated with mitochondria, J. Biol. Chem. 265 (1990) 7248–7256, https://doi.org/10.1016/S0021-9258(19)39106-9.
[105] C. Osman, D.R. Voelker, T. Langer, Making heads or tails of phospholipids in mitochondria, J. Cell Biol. 192 (2011) 7–16, https://doi.org/10.1083/jcb.201006159.
[106] C.-H. Wang, C.-H. Wang, P.-J. Hung, Y.-H. Wei, Disruption of mitochondria-associated ER membranes impairs insulin sensitivity and thermogenic function of adipocytes, Front Cell Dev. Biol. 10 (2022) 965523, https://doi.org/10.3389/fcell.2022.965523.
[107] J. Chen, A. Bassot, F. Giuliani, T. Simmen, Amyotrophic lateral sclerosis (ALS): stressed by dysfunctional mitochondria-endoplasmic reticulum contacts (MERCs), Cells 10 (2021) 1789, https://doi.org/10.3390/cells10071789.
[108] P. Morgado-Cáceres, G. Liabeuf, X. Calle, L. Briones, J.A. Riquelme, R. Bravo-Sagua, et al., The aging of ER-mitochondria communication: a journey from

undifferentiated to aged cells, Front Cell Dev. Biol. 10 (2022) 946678, https://doi.org/10.3389/fcell.2022.946678.
[109] P. Katti, S. Love-Rutledge, S.A. Murray, A. Hinton, Editorial: the role of mitochondrial endoplasmic reticulum contact sites in human health and disease, Front Mol. Biosci. 10 (2023) 1223354, https://doi.org/10.3389/fmolb.2023.1223354.
[110] L. Zhang, F. Yan, L. Li, H. Fu, D. Song, D. Wu, et al., New focuses on roles of communications between endoplasmic reticulum and mitochondria in identification of biomarkers and targets, Clin. Transl. Med. 11 (2021), https://doi.org/10.1002/ctm2.626.
[111] Y. Zhao, M. Zhang, W. Zhang, Y. Zhou, L. Chen, Q. Liu, et al., Isotropic super-resolution light-sheet microscopy of dynamic intracellular structures at subsecond timescales, Nat. Methods 19 (2022) 359–369, https://doi.org/10.1038/s41592-022-01395-5.
[112] S.C.J. Helle, Q. Feng, M.J. Aebersold, L. Hirt, R.R. Grüter, A. Vahid, et al., Mechanical force induces mitochondrial fission, ELife 6 (2017) e30292, https://doi.org/10.7554/eLife.30292.
[113] M. Brunstein, K. Wicker, K. Hérault, R. Heintzmann, M. Oheim, Full-field dual-color 100-nm super-resolution imaging reveals organization and dynamics of mitochondrial and ER networks, Opt. Express 21 (2013) 26162, https://doi.org/10.1364/OE.21.026162.
[114] F. Bottanelli, E.B. Kromann, E.S. Allgeyer, R.S. Erdmann, S. Wood Baguley, G. Sirinakis, et al., Two-colour live-cell nanoscale imaging of intracellular targets, Nat. Commun. 7 (2016) 10778, https://doi.org/10.1038/ncomms10778.
[115] B. Gottschalk, Z. Koshenov, O.A. Bachkoenig, R. Rost, R. Malli, W.F. Graier, MFN2 mediates ER-mitochondrial coupling during ER stress through specialized stable contact sites, Front Cell Dev. Biol. 10 (2022) 918691, https://doi.org/10.3389/fcell.2022.918691.
[116] K. Han, S. Huang, J. Kong, Y. Yang, L. Shi, Y. Ci, A novel fluorescent endoplasmic reticulum marker for super-resolution imaging in live cells, FEBS Lett. 597 (2023) 693–701, https://doi.org/10.1002/1873-3468.14581.
[117] M. Harner, C. Körner, D. Walther, D. Mokranjac, J. Kaesmacher, U. Welsch, et al., The mitochondrial contact site complex, a determinant of mitochondrial architecture: molecular architecture of mitochondria, EMBO J. 30 (2011) 4356–4370, https://doi.org/10.1038/emboj.2011.379.
[118] N. Pfanner, M. van der Laan, P. Amati, R.A. Capaldi, A.A. Caudy, A. Chacinska, et al., Uniform nomenclature for the mitochondrial contact site and cristae organizing system, J. Cell Biol. 204 (2014) 1083–1086, https://doi.org/10.1083/jcb.201401006.
[119] C. Ott, K. Ross, S. Straub, B. Thiede, M. Götz, C. Goosmann, et al., Sam50 functions in mitochondrial intermembrane space bridging and biogenesis of respiratory complexes, Mol. Cell. Biol. 32 (2012) 1173–1188, https://doi.org/10.1128/MCB.06388-11.
[120] C. Ding, Z. Wu, L. Huang, Y. Wang, J. Xue, S. Chen, et al., Mitofilin and CHCHD6 physically interact with Sam50 to sustain cristae structure, Sci. Rep. 5 (2015) 16064, https://doi.org/10.1038/srep16064.
[121] C.A. Mannella, M. Marko, P. Penczek, D. Barnard, J. Frank, The internal compartmentation of rat-liver mitochondria: tomographic study using the high-voltage transmission electron microscope, Microsc. Res Tech. 27 (1994) 278–283, https://doi.org/10.1002/jemt.1070270403.
[122] C.A. Mannella, D.R. Pfeiffer, P.C. Bradshaw, I.I. Moraru, B. Slepchenko, L. M. Loew, et al., Topology of the mitochondrial inner membrane: dynamics and bioenergetic implications, IUBMB Life 52 (2001) 93–100, https://doi.org/10.1080/15216540152845885.
[123] C. Frezza, S. Cipolat, O. Martins de Brito, M. Micaroni, G.V. Beznoussenko, T. Rudka, et al., OPA1 controls apoptotic cristae remodeling independently from mitochondrial fusion, Cell 126 (2006) 177–189, https://doi.org/10.1016/j.cell.2006.06.025.
[124] J. Tang, K. Zhang, J. Dong, C. Yan, C. Hu, H. Ji, et al., Sam50–Mic19–Mic60 axis determines mitochondrial cristae architecture by mediating mitochondrial outer and inner membrane contact, Cell Death Differ. 27 (2020) 146–160, https://doi.org/10.1038/s41418-019-0345-2.
[125] D.C. Jans, C.A. Wurm, D. Riedel, D. Wenzel, F. Stagge, M. Deckers, et al., STED super-resolution microscopy reveals an array of MINOS clusters along human mitochondria, Proc. Natl. Acad. Sci. USA 110 (2013) 8936–8941, https://doi.org/10.1073/pnas.1301820110.
[126] S. Stoldt, T. Stephan, D.C. Jans, C. Brüser, F. Lange, J. Keller-Findeisen, et al., Mic60 exhibits a coordinated clustered distribution along and across yeast and mammalian mitochondria, Proc. Natl. Acad. Sci. USA 116 (2019) 9853–9858, https://doi.org/10.1073/pnas.1820364116.
[127] P. Shi, X. Ren, J. Meng, C. Kang, Y. Wu, Y. Rong, et al., Mechanical instability generated by Myosin 19 contributes to mitochondria cristae architecture and OXPHOS, Nat. Commun. 13 (2022) 2673, https://doi.org/10.1038/s41467-022-30431-3.
[128] E.C. Genin, M. Plutino, S. Bannwarth, E. Villa, E. Cisneros-Barroso, M. Roy, et al., CHCHD10 mutations promote loss of mitochondrial cristae junctions with impaired mitochondrial genome maintenance and inhibition of apoptosis, EMBO Mol. Med 8 (2016) 58–72, https://doi.org/10.15252/emmm.201505496.
[129] L.D. Zorova, V.A. Popkov, E.Y. Plotnikov, D.N. Silachev, I.B. Pevzner, S. S. Jankauskas, et al., Mitochondrial membrane potential, Anal. Biochem. 552 (2018) 50–59, https://doi.org/10.1016/j.ab.2017.07.009.
[130] A.S. Monzel, J.A. Enríquez, M. Picard, Multifaceted mitochondria: moving mitochondrial science beyond function and dysfunction, Nat. Metab. 5 (2023) 546–562, https://doi.org/10.1038/s42255-023-00783-1.
[131] A.A. Amchenkova, L.E. Bakeeva, Y.S. Chentsov, V.P. Skulachev, D.B. Zorov, Coupling membranes as energy-transmitting cables. I. Filamentous mitochondria in fibroblasts and mitochondrial clusters in cardiomyocytes, J. Cell Biol. 107 (1988) 481–495, https://doi.org/10.1083/jcb.107.2.481.
[132] V.P. Skulachev, Mitochondrial filaments and clusters as intracellular power-transmitting cables, Trends Biochem. Sci. 26 (2001) 23–29, https://doi.org/10.1016/S0968-0004(00)01735-7.
[133] D.M. Wolf, M. Segawa, A.K. Kondadi, R. Anand, S.T. Bailey, A.S. Reichert, et al., Individual cristae within the same mitochondrion display different membrane potentials and are functionally independent, EMBO J. 38 (2019) e101056, https://doi.org/10.15252/embj.2018101056.
[134] B. Zhang, D. Wang, F. Guo, C. Xuan, Mitochondrial membrane potential and reactive oxygen species in cancer stem cells, Fam. Cancer 14 (2015) 19–23, https://doi.org/10.1007/s10689-014-9757-9.
[135] F. Vogel, C. Bornhövd, W. Neupert, A.S. Reichert, Dynamic subcompartmentalization of the mitochondrial inner membrane, J. Cell Biol. 175 (2006) 237–247, https://doi.org/10.1083/jcb.200605138.
[136] M. Strauss, G. Hofhaus, R.R. Schröder, W. Kühlbrandt, Dimer ribbons of ATP synthase shape the inner mitochondrial membrane, EMBO J. 27 (2008) 1154–1160, https://doi.org/10.1038/emboj.2008.35.
[137] M. Segawa, D.M. Wolf, N.W. Hultgren, D.S. Williams, A.M. van der Bliek, D. B. Shackelford, et al., Quantification of cristae architecture reveals time-dependent characteristics of individual mitochondria, Life Sci. Alliance 3 (2020) e201900620, https://doi.org/10.26508/lsa.201900620.
[138] C. Hu, L. Shu, X. Huang, J. Yu, liuju Li, L. Gong, et al., OPA1 and MICOS regulate mitochondrial crista dynamics and formation, Cell Death Dis. 11 (2020) 940, https://doi.org/10.1038/s41419-020-03152-y.
[139] A.K. Kondadi, R. Anand, S. Hänsch, J. Urbach, T. Zobel, D.M. Wolf, et al., Cristae undergo continuous cycles of membrane remodelling in a MICOS -dependent manner, EMBO Rep. 21 (2020) e49776, https://doi.org/10.15252/embr.201949776.
[140] D.M. Wolf, M. Segawa, O.S. Shirihai, M. Liesa, Method for live-cell super-resolution imaging of mitochondrial cristae and quantification of submitochondrial membrane potentials, in: Methods in Cell Biology, vol. 155, Elsevier,, 2020, pp. 545–555, https://doi.org/10.1016/bs.mcb.2019.12.006.
[141] S. Samanta, Y. He, A. Sharma, J. Kim, W. Pan, Z. Yang, et al., Fluorescent probes for nanoscopic imaging of mitochondria, Chem 5 (2019) 1697–1726, https://doi.org/10.1016/j.chempr.2019.03.011.
[142] C. Wang, M. Taki, Y. Sato, Y. Tamura, H. Yaginuma, Y. Okada, et al., A photostable fluorescent marker for the superresolution live imaging of the dynamic structure of the mitochondrial cristae, Proc. Natl. Acad. Sci. USA 116 (2019) 15817–15822, https://doi.org/10.1073/pnas.1905924116.
[143] X. Yang, Z. Yang, Z. Wu, Y. He, C. Shan, P. Chai, et al., Mitochondrial dynamics quantitatively revealed by STED nanoscopy with an enhanced squaraine variant probe, Nat. Commun. 11 (2020) 3699, https://doi.org/10.1038/s41467-020-17546-1.
[144] X. Li, T. Zhang, X. Diao, Y. Li, Y. Su, J. Yang, et al., Mitochondria-targeted fluorescent nanoparticles with large stokes shift for long-term bioimaging, Molecules 28 (2023) 3962, https://doi.org/10.3390/molecules28093962.
[145] L. Galluzzi, I. Vitale, S.A. Aaronson, J.M. Abrams, D. Adam, P. Agostinis, et al., Molecular mechanisms of cell death: recommendations of the Nomenclature Committee on Cell Death 2018, Cell Death Differ. 25 (2018) 486–541, https://doi.org/10.1038/s41418-017-0012-4.
[146] S.W. Lowe, E. Cepero, G. Evan, Intrinsic tumour suppression, Nature 432 (2004) 307–315, https://doi.org/10.1038/nature03098.
[147] L. Lossi, The concept of intrinsic versus extrinsic apoptosis, Biochem. J. 479 (2022) 357–384, https://doi.org/10.1042/BCJ20210854.
[148] R.J. Youle, A. Strasser, The BCL-2 protein family: opposing activities that mediate cell death, Nat. Rev. Mol. Cell Biol. 9 (2008) 47–59, https://doi.org/10.1038/nrm2308.
[149] M.C. Wei, W.-X. Zong, E.H.-Y. Cheng, T. Lindsten, V. Panoutsakopoulou, A. J. Ross, et al., Proapoptotic BAX and BAK: a requisite gateway to mitochondrial dysfunction and death, Science 292 (2001) 727–730, https://doi.org/10.1126/science.1059108.
[150] J.-C. Martinou, R.J. Youle, Mitochondria in apoptosis: Bcl-2 Family Members and Mitochondrial Dynamics, Dev. Cell 21 (2011) 92–101, https://doi.org/10.1016/j.devcel.2011.06.017.
[151] D. Kashyap, V.K. Garg, N. Goel, Intrinsic and extrinsic pathways of apoptosis: role in cancer development and prognosis, in: Advances in Protein Chemistry and Structural Biology, 125, Elsevier,, 2021, pp. 73–120, https://doi.org/10.1016/bs.apcsb.2021.01.003.
[152] N.S. Erekat, Apoptosis and its therapeutic implications in neurodegenerative diseases, Clin. Anat. 35 (2022) 65–78, https://doi.org/10.1002/ca.23792.
[153] X. Xu, Y. Lai, Z.-C. Hua, Apoptosis and apoptotic body: disease message and therapeutic target potentials, Biosci. Rep. 39 (2019) BSR20180992, https://doi.org/10.1042/BSR20180992.
[154] L. Große, C.A. Wurm, C. Brüser, D. Neumann, D.C. Jans, S. Jakobs, Bax assembles into large ring-like structures remodeling the mitochondrial outer membrane in apoptosis, EMBO J. 35 (2016) 402–413, https://doi.org/10.15252/embj.201592789.
[155] R. Salvador-Gallego, M. Mund, K. Cosentino, J. Schneider, J. Unsay, U. Schraermeyer, et al., Bax assembly into rings and arcs in apoptotic mitochondria is linked to membrane pores, EMBO J. 35 (2016) 389–401, https://doi.org/10.15252/embj.201593384.
[156] A. Rongvaux, R. Jackson, C.C.D. Harman, T. Li, A.P. West, M.R. de Zoete, et al., Apoptotic caspases prevent the induction of type I interferons by mitochondrial DNA, Cell 159 (2014) 1563–1577, https://doi.org/10.1016/j.cell.2014.11.037.

[157] M.J. White, K. McArthur, D. Metcalf, R.M. Lane, J.C. Cambier, M.J. Herold, et al., Apoptotic caspases suppress mtDNA-Induced STING-Mediated Type I IFN Production, Cell 159 (2014) 1549–1562, https://doi.org/10.1016/j.cell.2014.11.036.
[158] K. McArthur, L.W. Whitehead, J.M. Heddleston, L. Li, B.S. Padman, V. Oorschot, et al., BAK/BAX macropores facilitate mitochondrial herniation and mtDNA efflux during apoptosis, Science 359 (2018) eaao6047, https://doi.org/10.1126/science.aao6047.
[159] J.S. Riley, G. Quarato, C. Cloix, J. Lopez, J. O'Prey, M. Pearson, et al., Mitochondrial inner membrane permeabilisation enables mt DNA release during apoptosis, EMBO J. 37 (2018) e99238, https://doi.org/10.15252/embj.201899238.
[160] K. Cosentino, V. Hertlein, A. Jenner, T. Dellmann, M. Gojkovic, A. Peña-Blanco, et al., The interplay between BAX and BAK tunes apoptotic pore growth to control mitochondrial-DNA-mediated inflammation, 933-949.e9, Mol. Cell 82 (2022), https://doi.org/10.1016/j.molcel.2022.01.008.
[161] T. Appelhans, C.P. Richter, V. Wilkens, S.T. Hess, J. Piehler, K.B. Busch, Nanoscale organization of mitochondrial microcompartments revealed by combining tracking and localization microscopy, Nano Lett. 12 (2012) 610–616, https://doi.org/10.1021/nl203343a.
[162] V. Wilkens, W. Kohl, K. Busch, Restricted diffusion of OXPHOS complexes in dynamic mitochondria delays their exchange between cristae and engenders a transitory mosaic distribution, J. Cell Sci. 126 (2013) 103–116, https://doi.org/10.1242/jcs.108852.
[163] T. Appelhans, K.B. Busch, Dynamic imaging of mitochondrial membrane proteins in specific sub-organelle membrane locations, Biophys. Rev. 9 (2017) 345–352, https://doi.org/10.1007/s12551-017-0287-1.
[164] M. Bhagawati, T. Arroum, N. Webeling, A.G. Montoro, H.D. Mootz, K.B. Busch, The receptor subunit Tom20 is dynamically associated with the TOM complex in mitochondria of human cells, MBoC 32 (2021) br1, https://doi.org/10.1091/mbc.E21-01-0042.
[165] S.C.M. Reinhardt, L.A. Masullo, I. Baudrexel, P.R. Steen, R. Kowalewski, A. S. Eklund, et al., Ångström-resolution fluorescence microscopy, Nature 617 (2023) 711–716, https://doi.org/10.1038/s41586-023-05925-9.
[166] D. Choquet, M. Sainlos, J.-B. Sibarita, Advanced imaging and labelling methods to decipher brain cell organization and function, Nat. Rev. Neurosci. 22 (2021) 237–255, https://doi.org/10.1038/s41583-021-00441-z.
[167] D. Sage, T.-A. Pham, H. Babcock, T. Lukes, T. Pengo, J. Chao, et al., Super-resolution fight club: assessment of 2D and 3D single-molecule localization microscopy software, Nat. Methods 16 (2019) 387–395, https://doi.org/10.1038/s41592-019-0364-4.
[168] S. Fu, W. Shi, T. Luo, Y. He, L. Zhou, J. Yang, et al., Field-dependent deep learning enables high-throughput whole-cell 3D super-resolution imaging, Nat. Methods 20 (2023) 459–468, https://doi.org/10.1038/s41592-023-01775-5.
[169] A. Speiser, L.-R. Müller, P. Hoess, U. Matti, C.J. Obara, W.R. Legant, et al., Deep learning enables fast and dense single-molecule localization with high accuracy, Nat. Methods 18 (2021) 1082–1090, https://doi.org/10.1038/s41592-021-01236-x.
[170] A. Beghin, A. Kechkar, C. Butler, F. Levet, M. Cabillic, O. Rossier, et al., Localization-based super-resolution imaging meets high-content screening, Nat. Methods 14 (2017) 1184–1190, https://doi.org/10.1038/nmeth.4486.
[171] Q. Chen, C. Jin, X. Shao, R. Guan, Z. Tian, C. Wang, et al., Super-resolution tracking of mitochondrial dynamics with an iridium(III) luminophore, Small 14 (2018) 1802166, https://doi.org/10.1002/smll.201802166.
[172] Z. Ye, L. Wei, X. Geng, X. Wang, Z. Li, L. Xiao, Mitochondrion-specific blinking fluorescent bioprobe for nanoscopic monitoring of mitophagy, ACS Nano 13 (2019) 11593–11602, https://doi.org/10.1021/acsnano.9b05354.
[173] Y. Zhang, J. Wang, S. Xing, L. Li, S. Zhao, W. Zhu, et al., Mitochondria determine the sequential propagation of the calcium macrodomains revealed by the super-resolution calcium lantern imaging, Sci. China Life Sci. 63 (2020) 1543–1551, https://doi.org/10.1007/s11427-019-1659-4.
[174] S. Arai, M. Suzuki, S.-J. Park, J.S. Yoo, L. Wang, N.-Y. Kang, et al., Mitochondria-targeted fluorescent thermometer monitors intracellular temperature gradient, Chem. Commun. 51 (2015) 8044–8047, https://doi.org/10.1039/C5CC01088H.
[175] D. Chrétien, P. Bénit, H.-H. Ha, S. Keipert, R. El-Khoury, Y.-T. Chang, et al., Mitochondria are physiologically maintained at close to 50 °C, PLoS Biol. 16 (2018) e2003992, https://doi.org/10.1371/journal.pbio.2003992.
[176] X. Di, D. Wang, Q.P. Su, Y. Liu, J. Liao, M. Maddahfar, et al., Spatiotemporally mapping temperature dynamics of lysosomes and mitochondria using cascade organelle-targeting upconversion nanoparticles, Proc. Natl. Acad. Sci. USA 119 (2022) e2207402119, https://doi.org/10.1073/pnas.2207402119.
[177] M. Homma, Y. Takei, A. Murata, T. Inoue, S. Takeoka, A ratiometric fluorescent molecular probe for visualization of mitochondrial temperature in living cells, Chem. Commun. 51 (2015) 6194–6197, https://doi.org/10.1039/C4CC10349A.
[178] T.-B. Ren, S.-Y. Wen, L. Wang, P. Lu, B. Xiong, L. Yuan, et al., Engineering a reversible fluorescent probe for real-time live-cell imaging and quantification of mitochondrial ATP, Anal. Chem. 92 (2020) 4681–4688, https://doi.org/10.1021/acs.analchem.0c00506.
[179] F. Levet, E. Hosy, A. Kechkar, C. Butler, A. Beghin, D. Choquet, et al., SR-Tesseler: a method to segment and quantify localization-based super-resolution microscopy data, Nat. Methods 12 (2015) 1065–1071, https://doi.org/10.1038/nmeth.3579.
[180] F. Levet, G. Julien, R. Galland, C. Butler, A. Beghin, A. Chazeau, et al., A tessellation-based colocalization analysis approach for single-molecule localization microscopy, Nat. Commun. 10 (2019) 2379, https://doi.org/10.1038/s41467-019-10007-4.
[181] F. Levet, J.-B. Sibarita, PoCA: a software platform for point cloud data visualization and quantification, Nat. Methods 20 (2023) 629–630, https://doi.org/10.1038/s41592-023-01811-4.
[182] S.J. Sahl, S.W. Hell, High-Resolution 3D Light Microscopy with STED and RESOLFT, in: J.F. Bille (Ed.), High Resolution Imaging in Microscopy and Ophthalmology, Springer International Publishing, Cham, 2019, pp. 3–32, https://doi.org/10.1007/978-3-030-16638-0_1.